ELSEVIER

Process Biochemistry 40 (2005) 2263–2283

PROCESS BIOCHEMISTRY

www.elsevier.com/locate/procbio

Review

Bubble column reactors

Nigar Kantarci[a], Fahir Borak[b], Kutlu O. Ulgen[a,*]

[a]*Department of Chemical Engineering, Boğaziçi University, 34342 Bebek-Istanbul, Turkey*
[b]*Department of Chemical Engineering, Yeditepe University, 34755 Kadikoy-Istanbul, Turkey*

Received 31 August 2004; accepted 26 October 2004

Abstract

Bubble columns are intensively used as multiphase contactors and reactors in chemical, biochemical and petrochemical industries. They provide several advantages during operation and maintenance such as high heat and mass transfer rates, compactness and low operating and maintenance costs. Three-phase bubble column reactors are widely employed in reaction engineering, i.e. in the presence of a catalyst and in biochemical applications where microorganisms are utilized as solid suspensions in order to manufacture industrially valuable bioproducts. Investigation of design parameters characterizing the operation and transport phenomena of bubble columns have led to better understanding of the hydrodynamic properties, heat and mass transfer mechanisms and flow regime characteristics ongoing during the operation. Moreover, experimental studies are supported with computational fluid dynamics (CFDs) simulations and developed mathematical models to describe better the phenomena taking place in a bubble column reactor. This review focuses on bubble column reactors, their description, design and operation, application areas, fluid dynamics and regime analysis encountered and parameters characterizing the operation are presented together with the findings of published studies.

Keywords: Bubble columns; Bioreactors; Gas holdup; Heat transfer; Mass transfer; Fluid dynamics

Contents

* Corresponding author. Tel.: +90 212 359 6869; fax: +90 212 287 2460.
E-mail address: ulgenk@boun.edu.tr (K.O. Ulgen).

0032-9592/$ – see front matter © 2004 Elsevier Ltd. All rights reserved.
doi:10.1016/j.procbio.2004.10.004

1. Introduction

Bubble column reactors belong to the general class of multiphase reactors which consist of three main categories namely, the trickle bed reactor (fixed or packed bed), fluidized bed reactor, and the bubble column reactor. A bubble column reactor is basically a cylindrical vessel with a gas distributor at the bottom. The gas is sparged in the form of bubbles into either a liquid phase or a liquid–solid suspension. These reactors are generally referred to as slurry bubble column reactors when a solid phase exists. Bubble columns are intensively utilized as multiphase contactors and reactors in chemical, petrochemical, biochemical and metallurgical industries [1]. They are used especially in chemical processes involving reactions such as oxidation, chlorination, alkylation, polymerization and hydrogenation, in the manufacture of synthetic fuels by gas conversion processes and in biochemical processes such as fermentation and biological wastewater treatment [2,3]. Some very well known chemical applications are the famous Fischer–Tropsch process which is the indirect coal liquefaction process to produce transportation fuels, methanol synthesis, and manufacture of other synthetic fuels which are environmentally much more advantageous over petroleum-derived fuels [1].

Bubble column reactors owe their wide application area to a number of advantages they provide both in design and operation as compared to other reactors. First of all, they have excellent heat and mass transfer characteristics, meaning high heat and mass transfer coefficients. Little maintenance and low operating costs are required due to lack of moving parts and compactness. The durability of the catalyst or other packing material is high [1]. Moreover, online catalyst addition and withdrawal ability and plug-free operation are other advantages that render bubble columns as an attractive reactor choice [3]. Due to their industrial importance and wide application area, the design and scale-up of bubble column reactors, investigation of important hydrodynamic and operational parameters characterizing their operation have gained considerable attention during the past 20 years.

Recent research with bubble columns frequently focuses on the following topics: gas holdup studies [4–11], bubble characteristics [3,12–16], flow regime investigations and computational fluid dynamics studies [1,17–21], local and average heat transfer measurements [22–26], and mass transfer studies [27–31]. The effects of column dimensions, column internals design, operating conditions, i.e. pressure and temperature, the effect of superficial gas velocity, solid type and concentration are commonly investigated in these studies. Many experimental studies have been directed towards the quantification of the effects that operating conditions, slurry physical properties and column dimensions have on performance of bubble columns [32]. Although a tremendous number of studies exist in the literature, bubble columns are still not well understood due to the fact that most of these studies are often oriented on only one phase, i.e. either liquid or gas. However, the main point of interest should be the study of the interaction between the phases, which are in fact intimately linked [33].

1.1. Applications of bubble column reactors in bioprocesses

An important application area of bubble columns is their use as bioreactors in which microorganisms are utilized in order to produce industrially valuable products such as enzymes, proteins, antibiotics, etc. Several recent biochemical studies utilizing bubble columns as bioreactors are presented in Table 1. Arcuri et al. [34] using *Streptomyces*

Table 1
Biochemical applications of bubble column reactors

Bioproduct	Biocatalyst	Reference
Thienamycin	*Streptomyces cattleya*	[34]
Glucoamylase	*Aureobasidium pullulans*	[35]
Acetic acid	*Acetobacter aceti*	[36]
Monoclonal antibody	*Hybridoma cells*	[37]
Plant secondary metabolites	*Hyoscyamus muticus*	[38]
Taxol	*Taxus cuspidate*	[39]
Organic acids (acetic, butyric)	*Eubacterium limosum*	[40]
Low oxygen tolerance	*Arabidopsis thaliana*	[41]
Ethanol fermentation	*Saccharomyces cerevisiae*	[42]

cattleya, studied the production of thienamycin with continuously operated bubble column bioreactor. Federici et al. [35] performed the production of glucoamylase by *Aureobasidium pullulans*. Sun and Furusaki [36] investigated the production of acetic acid in a bubble column by using *Acetobacter aceti*. Rodrigues et al. [37] reported that the cultivation of hybridoma cells in a bubble column reactor resulted in a high monoclonal antibody productivity of 503 μg/l day. Bordonaro and Curtis [38] designed a 15 l bubble column reactor to produce root cultures of *Hyoscyamus muticus* which in turn produces plant secondary metabolites. Son et al. [39] developed a novel bubble column bioreactor to produce taxol by *Taxus cuspidate* and inoculated the cells in various type of bioreactors to test growth performance. Chang et al. [40] cultivated *Eubacterium limosum* on carbon monoxide to produce organic acids in a bubble column reactor. Shiao et al. [41] investigated the tolerance of *Arabidopsis thaliana* hairy roots to low oxygen conditions in a bubble column reactor. A recent study that was not aimed to produce a bioproduct but instead, investigate the hydrodynamic and heat transfer characteristics of the bubble column in the presence of microorganisms has been carried out by Prakash et al. [3]. They utilized a suspension of yeast cells (*Saccharomyces cerevisiae*) as the solid phase in an air–water system. The study of Ogbonna et al. [42] was based on the potential of producing fuel ethanol from sugar beet juice in a bubble column. In this study yeast cells (*Saccharomyces cerevisiae*) were used in order to investigate the feasibility of scaling up the process.

The present review covers basic concepts related to bubble column reactors such as design and scale-up, fluid dynamics and regime analysis, and important parameters characterizing their operation by reviewing the findings of several selected published works over the last 20 years. A summary of system properties and remarks on several studies reviewed is presented in Table 2.

2. Bubble column reactors: concepts and published work

As far as published studies are concerned, the main interest is concentrated on design and scale-up, fluid dynamics and regime analysis and characteristic parameters, especially gas holdup, bubble characteristics, mass transfer coefficient and heat transfer coefficient. In this section, together with these concepts, the effects of superficial gas velocity, liquid properties, operating conditions, column dimensions, gas distributor design, solid type and concentrations are presented.

2.1. Design and scale-up

The design and scale-up of bubble columns have gained considerable attention in recent years due to complex hydrodynamics and its influence on transport characteristics. Although the construction of bubble columns is simple, accurate and successful design and scale-up require an improved understanding of multiphase fluid dynamics and its influences. Industrial bubble columns usually operate with a length-to-diameter ratio, or aspect ratio of at least 5 [1]. In biochemical applications this value usually varies between 2 and 5. The effects brought about by the selection of column dimensions have found interest in bubble column reactor design. First, the use of large diameter reactors is desired because large gas throughputs are involved. Additionally large reactor heights are required to obtain large conversion levels [43]. However, there are also disadvantages brought about by the use of large diameter and tall columns in terms of ease of operation. As a result it is necessary to talk about an optimization process for best output. Generally two types of mode of operation are valid for bubble columns, namely the semibatch mode and continuous mode. In continuous operation, the gas and the suspension flow concurrently upward into the column and the suspension that leaves the column is recycled to the feed tank. The liquid superficial velocity is maintained to be lower than the gas superficial velocity by at least an order of magnitude. However, in the semibatch mode the suspension is stationary, meaning zero liquid throughputs, and the gas is bubbled upward into the column [32].

The design and scale-up of bubble column reactors generally depend on the quantification of three main phenomena: (i) heat and mass transfer characteristics; (ii) mixing characteristics; (iii) chemical kinetics of the reacting system. Thus, the reported studies emphasize the requirement of improved understanding of the multiphase fluid dynamics and its influence on phase holdups, mixing and transport properties [1]. Scale-up problems basically stem from the scale-dependency of the fluid dynamic phenomena and heat and mass transfer properties. Scale-up methods used in biotechnology and chemical industry range from know-how based methods that are in turn based on empirical guidelines, scale-up rules and dimensional analysis to know-why based approaches that should begin with regime analysis. The regime analysis is then followed by setting-up appropriate models that may be simplified to deal with the complex hydrodynamics [44].

Table 2
Summary of the system properties of several literature studies reviewed

Investigator	System	Column-gas distributor	Gas velocity (cm/s)	Parameters investigated
Deckwer et al. [60]	Nitrogen–molten paraffin-catalyst particles (Fischer–Tropsch process), 5 μm powdered Al_2O_3 catalyst particles concentration up to 16% (w/w)	4.1 and 10 cm i.d. column, perforated plate sparger with 75 μm hole diameters	Up to 4	Gas holdup, heat transfer
Schumpe and Grund [48]	Air–water	0.3 m i.d. column, ring distributor with 1 mm holes	Up to 20	Gas holdup, bubble characteristics
Ozturk et al. [70]	Organic liquids (ethylbenzene, ethylacetate, decalin, acetone, nitrobenzene, toluene, ethanol)–air	9.5 cm i.d. column, single tube sparger with 3 mm diameter holes	0.8–10	Gas holdup, mass transfer
Saxena et al. [63]	Air–water and air–water–glass beads, glass beads of 50, 90, 143.3 μm diameter, up to 20% (w/w) concentration	30.5, 10.8 cm i.d columns, perforated plate sparger	Up to 28	Gas holdup, bubble characteristics
Daly et al. [64]	Nitrogen–molten wax (paraffin wax and wax produced by Fischer–Tropsch reactor)	5 and 21 cm i.d. columns, perforated plate distributor with 2 mm hole diameters	Up to 12	Gas holdup, bubble characteristics
Pino et al. [32]	Air–kerosene-four different solid particles, with 1.5, 5, 90, 135 μm diameters, concentration between 0 and 500 kg/m^3	29 and 10 cm i.d. columns, perforated plate distributor with 3 mm hole diameters	Up to 15	Gas holdup
Krishna et al. [57]	Water–air, helium, argon and sulfur hexafluoride	5 and 10 cm i.d. columns, sintered plate distributor		Transition gas velocity and holdup, bubble rise velocities and bubble holdup
Li and Prakash [68]	Air–water–glass beads of 35 μm diameter and concentration up to 40% (v/v)	0.28 m i.d. column, 6-arm distributor with 1.5 mm diameter holes	5–35	Gas holdup
Hyndman et al. [45]	Air–water and air + argon–water	20 cm i.d. column, perforated plate sparger with 1 mm hole diameters	1.9–15.4	Gas holdup, bubble characteristics
Krishna et al. [43]	Air–parafinic oil–silica particles, concentration up to 36% (v/v), with size distribution: 10% < 27 μm; 50% < 38 μm; 90% < 47 μm	10–19–38 cm i.d. columns, perforated plate sparger with 50 μm hole diameters		Gas holdup, bubble characteristics
Luo et al. [4]	Paratherm NF heat transfer fluid-nitrogen gas–alumina particles, particle diameter 100 μm with solids volume fractions up to 0.19	10.2 cm column i.d., perforated plate sparger with 1.5 mm hole diameters	Up to 45	Gas holdup, bubble characteristics (bubble sizes, rise velocity and holdup)
Li and Prakash [13]	Air–water–glass beads, 35 μm glass beads of concentration up to 40% (v/v)	0.28 m i.d. column, 6-arm sparger with 1.5 mm hole diameters	5–35	Gas holdup, bubble characteristics, heat transfer
Lefebvre and Guy [33]	Air–water	20 cm i.d. column, perforated plate sparger with 69.1 mm hole diameters	0.9–7.8	Liquid velocity profiles, bubble velocity distributions
Li and Prakash [14]	Air–water and Air–water–glass beads, 35 μm glass beads of concentration up to 40% (v/v)	0.28 m i.d. column, 6-arm sparger with 1.5 mm hole diameters	5–35	Gas holdup, bubble characteristics
Prakash et al. [3]	Air–water–yeast cells, with 8 μm yeast cells of concentration 0–0.4% (w/w)	28 cm i.d. column, 6-arm sparger with 1.5 mm hole diameters	5–30	Gas holdup, bubble characteristics, heat transfer
Bouafi et al. [5]	Air–water	15 and 20 cm i.d. columns, perforated plate sparger with 2.5 mm, porous plate sparger with 0.3 porosity, membrane sparger with 0.5 mm hole diameters	2.5–4	Gas holdup, bubble sizes, mass transfer, axial liquid dispersion
Degaleesan et al. [1]	Air–water	14–19 and 44 cm i.d. columns, perforated plate spargers with 0.33, 0.4, 0.7 and 1 mm hole diameters and bubble cap distributor with 5 mm diameter holes	Up to 12	Fluid dynamics, liquid velocity profiles, gas holdup

Behkish et al. [27]	Organic liquid mixtures (isopar-M and hexanes mixtures) with four different gas phases (H_2, CO, N_2, CH_4) and two different solids (iron oxides and glass beads)	31.6 cm i.d. column	8–20	Mass transfer
Lapin et al. [16]	Air–water	30 cm i.d. column, ring sparger with 1 mm diameter holes	Fixed at 1	Bubble size distributions, bubble velocity profiles, flow structures
Cho et al. [25]	Viscous liquid medium (viscosity up to 38 mPa s) – air	15.2 cm i.d. column, perforated plate sparger	Up to 12	Heat transfer
Maalej et al. [29]	Aqueous solution of Na_2NO_3–$NaHCO_3$ and CO_2–N_2	4.6 cm i.d. column, perforated plate spargers with 2 mm diameter holes	Up to 3	Liquid and gas phase mass transfers
Verma and Rai [28]	Ferro-ferricyanide (electrolytic solution)–air	5.15 cm i.d. column, single-nozzle sparger with 1, 1.5 and 2 mm diameter holes	Up to 3.5	Gas holdup, mass transfer
Forret et al. [9]	Air–water	10–40 and 100 cm i.d. columns	5–20	Liquid velocity and mixing measurements, gas holdup
Chen et al. [26]	Air–water	20–40 and 80 cm i.d. columns, perforated plate spargers with 0.5 mm diameter holes	2–9	Local heat transfer measurements
Krishna and Van Baten [30]	Air–water	10–38 and 100 cm i.d. columns	10–38	CFD simulations, bubble properties, mass transfer
Vandu and Krishna [31]	Liquid phases (water, tetradecane, paraffin oil and tellus oil)–air–porous silica particles of 35 μm diameter and concentration up to 25% (v/v)	10 cm i.d. column, 8-arm sparger with 2.5 mm hole diameter and siever plate spargers with hole diameter 0.5 mm	Up to 40	Mass transfer
Thorat and Joshi [21]	Water, aqueous solution of NaCl (0.2 M) and aqueous solution of carboxy methyl cellulose (1%, w/w)–air	38.5 cm i.d. column, perforated plate type 20 different spargers with hole diameter range 0.8–50 mm	Up to 30	Fluid dynamics and regime transition
Veera et al. [11]	Aqueous solution of *n*-butanol–air	38.5 cm i.d. column, perforated plate spargers with 1 mm diameter	6–24	Radial gas holdup profiles
Tang and Heindel [10]	Air–water	15.24 cm i.d. column, 8-arm sparger with 1.6 mm diameter holes	Up to 20	Time-dependent gas holdup variation
Dhotre et al. [20]	Water, aqueous solution of *n*-butanol, carboxy methyl cellulose–air	38.5 cm i.d., perforated plate spargers with hole diameter range 0.8–87 mm	Up to 32.4	CFD simulations, radial gas holdup profiles

More specifically, in order to design bubble column reactors, the following hydrodynamic parameters are required: specific gas–liquid interfacial area, axial solids dispersion coefficients, sauter mean bubble diameter, axial dispersion coefficients of the gas and liquid, overall heat transfer coefficient between slurry and immersed heat transfer internals, mass transfer coefficients for all the species, gas holdups, physicochemical properties of the liquid medium. In order to estimate these design parameters for the system, experimental studies benefit from specialized measuring devices and accessories. The gas flow into the column is measured via rotameter and the superficial gas velocity is adjusted. The gas is distributed by a gas distributor, which has different alternatives such as ring type, perforated plate or arm distributor. An electric heater can be installed to maintain constant temperature in the column. The pressure measurement system may contain liquid manometers or pressure transducers (pressure transmitters). Pressure measurements are used to estimate gas holdup in the system. Thermocouples are used wherever temperature variation is needed to be recorded. Heat flux sensors may be used to estimate the heat flux and to measure the corresponding heat transfer coefficients between the heated immersed object and slurry or the slurry and wall. For better control and adjustment, the equipments are usually accompanied by PID controllers. Data acquisition systems may be utilized for instantaneous parameter investigations, for instance for recording the pressure fluctuations and estimation of instantaneous gas holdups and bubble properties.

2.2. Fluid dynamics and regime analysis

The fluid dynamic characterization of bubble column reactors has a significant effect on the operation and performance of bubble columns. According to literature, the experimental results obtained by parameter investigations, strictly depend on the regime prevailing in the column. The flow regimes in bubble columns are classified and maintained according to the superficial gas velocity employed in the column. Three types of flow regimes are commonly observed in bubble columns which are the homogeneous (bubbly flow) regime; the heterogeneous (churn-turbulent) regime and slug flow regime [45]. There also exists the so-called ‘‘foaming regime’’ which is not so commonly encountered in bubble columns.

The bubbly flow regime, also called the homogeneous flow regime is obtained at low superficial gas velocities, approximately less than 5 cm/s in semibatch columns [46,47]. This flow regime is characterized by bubbles of relatively uniform small sizes and rise velocities [48]. A uniform bubble distribution and relatively gentle mixing is observed over the entire cross-sectional area of the column [45]. There is practically no bubble coalescence or break-up, thus bubble size in this regime is almost completely dictated by the sparger design and system properties [21]. Kawagoe et al. [49] found that the gas holdup in the bubbly flow regime increases linearly with increasing superficial gas velocity.

The churn-turbulent regime, also called the heterogeneous regime is maintained at higher superficial gas velocities (greater than 5 cm/s in batch columns). This regime is characterized by the disturbed form of the homogeneous gas–liquid system due to enhanced turbulent motion of gas bubbles and liquid recirculation. As a result unsteady flow patterns and large bubbles with short residence times are formed by coalescence due to high gas throughputs. This flow regime is thus sometimes referred as coalesced bubble flow regime, indicating the much different sizes of the bubbles [48]. As a matter of fact, by bubble coalescence and break-up, a wide bubble size distribution is attained. The average bubble size is governed by coalescence and break-up which is controlled by the energy dissipation rate in the bulk [21]. Vigorous mixing, bubble cluster formation and wide bubble size range were also pointed out by Hyndman et al. [45]. Matsuura and Fan [50] reported that this regime consisted of a mixture of small and larger bubbles with diameters ranging from a few millimeters to a few centimeters. Recently coalescence and break-up have been studied numerically by solving related transport equations [51–54]. Churn-turbulent flow is frequently observed in industrial-size, large diameter columns [45]. It has been shown that the gas–liquid mass transfer coefficient is lower at churn-turbulent (heterogeneous) regime as compared to homogeneous flow. However, despite this fact, bubble columns are mostly operated under heterogeneous flow conditions in the chemical industry and the interpretations of effective interfacial area measurements, the design parameter estimations and reactor modeling concepts have been based on the assumption of two distinct bubble classes [48]. For these models, information on the holdup fractions, contributions to the overall flow, rise velocity and superficial gas velocity fractions are required for small and large bubbles.

A slug flow regime has been only observed in small diameter laboratory columns at high gas flow rates [45]. This regime takes its name from the formation of bubble slugs when larger bubbles are stabilized by the column wall. Hills [55] and Miller [56] reported that bubble slugs have been observed in the column diameter up to 15 cm. Fig. 1 best illustrates the differences between the possible regimes discussed.

The detection of regime transition from homogeneous to churn-turbulent flow and the investigation of the transition regime are quite important. As the transition takes place, significant changes are observed in the hydrodynamic behaviour of the system. There exists an onset of upward liquid circulation in the column centre and downward liquid circulation near the column wall. As a result more gas entry takes place in the centre, leading to build-up of transverse holdup-profile that enhances liquid circulation. Recently,

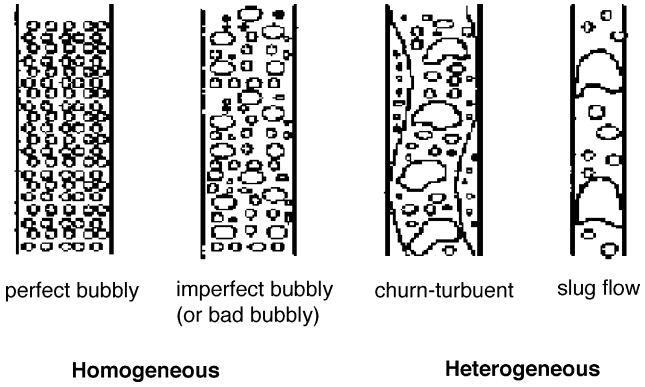

Fig. 1. Schematic of possible flow regimes in bubble columns [5].

Thorat and Joshi [21] reported that the transition gas velocity depends on column dimensions (diameter, dispersion height), sparger design and physical properties of the system. However, the effects of these parameters have not been investigated thoroughly in literature so far. The authors also analyzed the critical gas holdup, i.e. transition holdup and concluded that the critical gas holdup increased with decreasing aspect ratio and sparger hole diameter. Krishna et al. [57] investigated the influence of gas density on regime transition. They reported that the regime transition velocity increased with increasing gas density.

In order to characterize the flow regimes, unfortunately it is not possible to give definite quantitative ranges for superficial velocities. Different studies performed with different systems and operating conditions provide different results in determination of regime boundaries and regime transitions. For instance Hyndman et al. [45] proposed that below 4 cm/s superficial velocity a bubbly flow regime prevails. Pino et al. [32] also reported approximately the same velocity for a bubbly flow regime. Schumpe and Grund [48] proposed that for superficial velocities lower than 5 cm/s, homogeneous (bubbly) flow prevails. Bukur and Daly [58] observed the churn-turbulent flow regime for gas superficial velocities between 2 and 5 cm/s. Several flow regime charts have been presented in literature to identify the boundaries of possible flow regimes [2,59,60]. In Fig. 2, one such flow regime map presented by Deckwer et al. [60] is shown. The map describes quantitatively the dependence of flow regimes on column diameter and superficial gas velocity and is valid for both bubble and slurry bubble columns with a batch (stationary) liquid phase operated with a low viscosity liquid phase. The shaded regions in the figure indicate the transition regions between various flow regimes. However, the exact boundaries associated with the transition regions would depend on the system studied.

Table 3
Experimental values of transition velocity and gas holdup for air–water system bubble columns [95]

Research group	$V_{g,trans}$ (m/s)	$\varepsilon_{g,trans}$
Bach and Pilhofer [96]	0.046	0.277
Oels et al. [97]	0.039	0.178
Krishna et al. [72]	0.033	0.198
Yamashita and Inoue [98]	0.040	0.234
Hyndman et al. [45]	0.037	0.137

Hyndman et al. [45] reported that the transition from bubbly to churn-turbulent flow in a bubble column with increasing superficial gas velocity is in reality a gradual process. However, when modeling the complex hydrodynamics of bubble columns the simplification of the gradual process by defining a transition point is useful for modeling the hydrodynamic behaviour. Table 3 lists the results of the literature studies with an air–water system for the regime transition properties.

2.3. Gas holdup

Gas holdup is a dimensionless key parameter for design purposes that characterizes transport phenomena of bubble

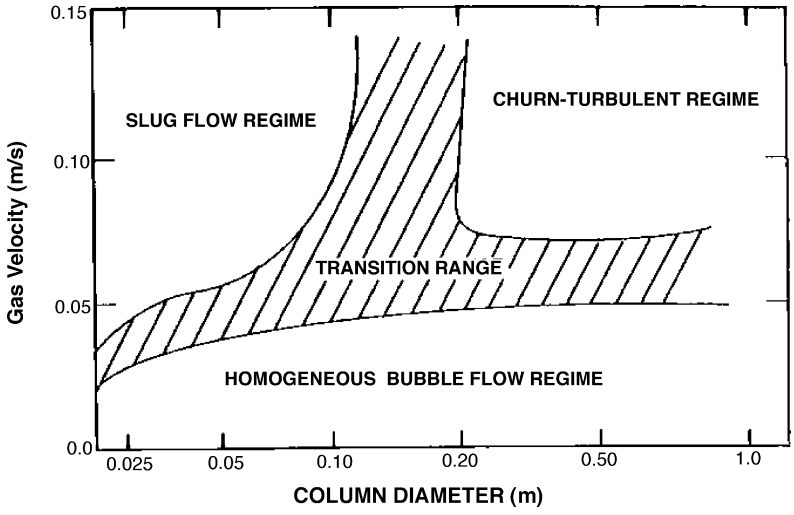

Fig. 2. Flow regime map for bubble columns [60].

column systems [4]. It is basically defined as the volume fraction of gas phase occupied by the gas bubbles. Likewise it is possible to characterize the liquid and solid phase holdups as the volume fraction of liquid and solid phases, respectively. All studies examine gas holdup because it plays an important role in design and analysis of bubble columns. As reported by Li and Prakash [14], in a three-phase slurry bubble column, the static pressure drop along the bed height can be expressed as

$$\Delta P = (\rho_g \varepsilon_g + \rho_l \varepsilon_l + \rho_s \varepsilon_s) g \Delta H \quad (1)$$

In the above equation, ε_g, ε_l and ε_s are the volume fractions of gas, liquid and solid phases, respectively. ε_g is also named as the gas holdup, g, ρ and ΔH are the gravitational acceleration, the density and height difference between the transducers, respectively. The subscripts g, l and s stands for gas, liquid and solid phases. By proper substitutions, starting with Eq. (1), one can factor out the gas holdup as

$$\varepsilon_g = 1 - \frac{1}{g(\rho_l \phi_l + \rho_s \phi_s)} \frac{\Delta P}{\Delta H} \quad (2)$$

Eq. (2) can be directly applied for estimation of gas holdup in a slurry bubble column. The most widely used technique in estimating gas holdup is the pressure profile method which is based on measuring the static pressure at two or more points along the column using manometers or more recently pressure transducers and thus obtaining the pressure drop, ΔP, along the bed [56,59,61,62].

The spatial variation of gas holdup, i.e gas holdup profile is another important factor which gives rise to pressure variation and thus liquid recirculation. Since liquid recirculation plays an important role in mixing and heat and mass transfer, predictions of radial gas holdup profiles would lead to better understanding of these phenomena and thus more reliable bubble column scale-up. The magnitude of gas holdup radial gradients depends on superficial gas velocity, column diameter, physical properties of the system and operating conditions [51]. There exist various correlations in literature in order to predict the gas holdup in both two-phase bubble columns and three-phase slurry bubble columns. In Table 4, several frequently used gas holdup correlations for bubble and slurry bubble columns are summarized.

It is reported that the basic factors affecting gas holdup are: superficial gas velocity, liquid properties, column dimensions, operating temperature and pressure, gas distributor design, solid phase properties. In the subsections below, the findings of various studies on the effects of these factors are presented.

2.3.1. Superficial gas velocity

Superficial gas velocity is the average velocity of the gas that is sparged into the column which is simply expressed as the volumetric flow rate divided by the cross-sectional area of the column. Gas holdup in bubble columns depends mainly on superficial gas velocity [2]. For both bubble columns and slurry bubble columns, gas holdup has been found to increase with increasing superficial gas velocity [3,14,32,43,45,48,60,63,64]. Although the systems investigated in these studies are quite different from each other, all conclude that the gas holdup increases with increasing superficial gas velocity. This increase has been found to be proportional to superficial gas velocity in the bubbly flow regime [65,66]. For the churn-turbulent regime, the effect of superficial velocity on gas holdup is less pronounced [66,67]. Hyndman et al. [45] analyzed the contribution of small and large bubbles to overall holdup via equations. The authors pointed out that in the churn-turbulent regime, as the superficial velocity increases the overall holdup increases due to the large bubble holdup increase. The contribution of small bubbles to overall holdup is constant and equal to the transition holdup, i.e. it does not increase with increasing superficial velocity. But the large bubble holdup increases with increasing superficial velocity, leading to the increase of the overall holdup. However, in bubbly flow, small bubble holdup is not constant but changes significantly as the superficial velocity is changed. Recently Veera et al. [11] reported an experimental study based on investigation of effect of gas velocity on gas holdup profiles in foaming liquids. They observed that the superficial gas velocity has a large influence on radial holdup profile at high foaming agent concentrations.

2.3.2. Liquid phase properties

The liquid phase property has an impact on bubble formation and/or coalescing tendencies and hence is an important factor affecting gas holdup. An increase in liquid viscosity results in large bubbles and thus higher bubble rising velocities and lower gas holdup [68]. It is also reported that adding a small amount of a surface acting material (surfactant) to water, results in significantly higher gas holdup values. Moreover, the presence of electrolyte or impurities also increases gas holdup [61,69]. Ozturk et al. [70] investigated the gas holdups in various organic liquids and they reported that in several mixed and adjusted mixtures, the gas holdups were higher as compared to pure liquids with the same properties (surface tension, density, viscosity). They also concluded that the gas holdups were higher with high density gases. Veera et al. [11] investigated gas holdup in the presence of foaming liquids and concluded that the effect of foaming agent concentration on holdup profiles depended upon the sparger design, column aspect ratio and superficial gas velocity. The authors also claimed that the gas holdup profiles were flatter at higher foaming agent concentrations. Recently, Tang and Heindel [10] suggested that regular tap water, which is the most frequently used liquid in bubble columns, might cause significant reproducibility problems in air–water two phase studies. They observed time-dependent variation of gas holdup which was then related to water quality, column operation mode, sparger orientation and superficial gas and liquid velocities. They attributed this time-dependency to coalescence inhibition caused by the existence of volatile substances present in tap water.

Table 4
Gas holdup correlations for bubble columns

Research group	Correlation	Reference
Joshi and Sharma [99]	$\varepsilon_g = \frac{V_g}{0.3+2V_g}$	[99]
Lockett and Kirkpatrick [65]	$V_g(1-\varepsilon_g) + V_l\varepsilon_g = V_b\varepsilon_g(1-\varepsilon_g)^{2.39}(1+2.55\varepsilon_g^3)$	[65]
Koide et al. [79]	$\varepsilon_g = \frac{V_g}{31+\beta(1-e)\sqrt{V_g}}$, $\beta = 4.5 - 3.5\exp(-0.064D_T^{1.3})$; $e = -\frac{0.18V_g^{1.8}}{\beta}$	[79]
Sada et al. [69]	$\varepsilon_g = 0.32(1-\varepsilon_g)^4 Bo^{0.21}Ga^{0.086}Fr(\rho_g/\rho_l)^{0.068}$	[63]
Kumar et al. [100]	$\varepsilon_g = 0.728U' - 0.485U'2 + 0.0975U'3$, $U' = V_g[\rho_l^2/\{\sigma_l(\rho_l-\rho_g)g\}]^{1/4}$	[63]
Grover et al. [101]	$\varepsilon_g = \left(\frac{1+aP_v}{bP_v}\right)\left(\frac{V_g\mu_l}{\sigma_l}\right)^{0.76}\left(\frac{\mu_l^4 g}{\rho_l\sigma_l^3}\right)^{-0.27}\left(\frac{\rho_g}{\rho_l}\right)^{0.09}\left(\frac{\mu_g}{\mu_l}\right)^{0.35}$, $a = 1.1\times10^{-4}$ and $b = 5\times10^{-4}$	[63]
Zou et al. [102]	$\varepsilon_g = 0.17283\left(\frac{\mu_l^4 g}{\rho_l\sigma_l^3}\right)^{-0.15}\left(\frac{V_g\mu_l}{\sigma_l}\right)^{0.58}\left(\frac{P+P_v}{P}\right)^{1.61}$	[63]
Hughmark [103]	$\varepsilon_g = \frac{1}{2+(0.35/V_g)(\rho_l\sigma/72)^{1/3}}$	[6]
Kawase and Moo-Young [87]	$\varepsilon_g = 1.07Fr^{1/3}$	[87]
Kawase et al. [104]	$\frac{\varepsilon_g}{1+\varepsilon_g} = 0.0625\left(\frac{V_g}{\upsilon_l g}\right)^{1/4}$	[6]
Akita and Yoshida [77]	$\frac{\varepsilon_g}{(1-\varepsilon_g)^4} = \alpha\left(\frac{d_R^2\rho_l g}{\sigma}\right)^{1/8}\left(\frac{gd_R^3\rho_l^2}{\mu_l^2}\right)^{1/12}\frac{V_g}{\sqrt{gd_R}}$, first term: Bond number, second term: Galilei number, third term: Froude number, $\alpha = 0.2$ for pure liquids and non-electrolyte solutions, $\alpha = 0.25$ for salt solutions	[44]
Hikita and Kikukawa [105]	$\varepsilon_g = 0.505V_g^{0.47}\left(\frac{0.072}{\sigma}\right)^{2/3}\left(\frac{0.001}{\mu_l}\right)^{0.05}$	[70]
Hikita et al. [61]	$\varepsilon_g = 0.672f\left(\frac{u_g\mu_l}{\sigma}\right)^{0.578}\left(\frac{\mu_l^4 g}{\rho_l\sigma^3}\right)^{-0.131}\left(\frac{\rho_g}{\rho_l}\right)^{0.062}\left(\frac{\mu_g}{\mu_l}\right)^{0.107}$, $f = 1$ for pure liquids and non-electrolyte solutions for ionic solutions f is a function of ionic strength	[44]
Reilley et al. [62]	$\varepsilon_g = 0.009 + 296V_g^{0.44}(\rho_l \text{ or } \rho_{sl})^{-0.98}\sigma_l^{-0.16}\rho_g^{0.19}$	[63]
Godbole et al. [106]	$\varepsilon_g = 0.239V_g^{0.634}d_R^{-0.5}$, for viscous media in slug flow regime	[44]
Sada et al. [69]	$\frac{\varepsilon_g}{(1-\varepsilon_g)^3} = 0.019V_\infty^{1/16}\upsilon_s^{-0.125V_\infty^{-0.16}}V_g$	[69]
Schumpe and Deckwer [107]	$\varepsilon_g = 0.2\left(\frac{d_R^2\rho_l g}{\sigma}\right)^{-0.13}\left(\frac{gd_R^3\rho_l^2}{\mu_{eff}^2}\right)^{0.11}\left(\frac{V_g}{\sqrt{gd_R}}\right)^{0.54}$ used for highly viscous media and groups vary in the following ranges: $1.4\times10^3 \le Bo \le 1.4\times10^5$, $1.2\times10^7 \le Ga \le 6.5\times10^{10}$, $3\times10^{-3} \le Fr \le 2.2\times10^{-1}$	[44]
Smith et al. [108]	$\varepsilon_g = \left[2.25 + \frac{0.379}{V_g}\left(\frac{\rho_l \text{ or } \rho_{sl}}{72}\right)^{0.31}(\mu_l \text{ or } \mu_{sl})^{0.016}\right]^{-1}$, $\mu_{sl} = \mu_l\exp\left[\frac{(5/3)\upsilon_s}{1-\upsilon_s}\right]$	[63]
Roy et al. [109]	$\varepsilon_g = 3.88\times10^{-3}\left[Re_T\left(\frac{\sigma_w}{\sigma_l}\right)^{1/3}(1-\upsilon_s)^3\right]^{0.44}$, for $Re_T > 500$, $\upsilon_s = \frac{W_s/\rho_s}{(W_s/\rho_s)+(W_l/\rho_l)}$	[63]
Koide et al. [67]	$\frac{\varepsilon_g}{(1-\varepsilon_g)^4} = \frac{k_l(V_g\mu_l/\sigma_l)^{0.918}}{1+4.35\upsilon_s^{0.748}[(\rho_s-\rho_l)/\rho_l]^{0.88}}\frac{(g\mu_l^4/(\rho_l\sigma_l^3))^{-0.252}}{(D_cV_g/\rho_l)^{-0.168}}$	[67]

2.3.3. Operating conditions

The effect of operating pressure and temperature on gas holdup of bubble columns were also investigated in many studies [44,62,57,71–73]. It is commonly accepted that elevated pressures lead to higher gas holdups. Empirical correlations have been proposed for gas holdup in bubble columns operated at high pressure and temperature [62,71]. Luo et al. [4] carried out experiments at about 5.6 MPa, to investigate the effect of pressure on the hydrodynamics of a slurry bubble column and found that gas holdup increases with pressure and the pressure effect is more pronounced in higher concentration slurries. In the study of Deckwer et al. [60] typical high pressure conditions of the Fischer–Tropsch process were investigated, i.e. 400–1100 kPa. However, they concluded that pressure had no significant effect on holdup. The operating temperature is another important factor to be discussed. Although most studies conclude that the temperature effect is not so significant, some disagree with this argument. For instance, Deckwer et al. [60] reported a decrease in the gas holdup with increasing temperature up to a certain temperature value and the gas holdup had reached a constant value with further increase of temperature. An interesting point in this study was that these results were obtained in a small diameter column, suggesting that in larger diameter columns, such a temperature effect would not be observed. Thus, the authors attributed this trend to possible ''wall effects'' in the small diameter column. Saxena et al. [63] investigated two and three-phase bubble columns within a 297–343 K temperature range and they found out such a

temperature dependence of gas holdup only in the two-phase system.

2.3.4. Column dimensions

The effect of column diameter and height on hydrodynamics is also widely investigated in literature. Shah et al. [2] reported that in bubble columns, the effect of column size on gas holdup is negligible when the column diameter is larger than 10–15 cm. Luo et al. [4] reported that the influence of the column height is insignificant if the height is above 1–3 m and the ratio of the column height to the diameter (aspect ratio) is larger than 5. Possible wall effects brought about by the use of small diameter columns ($\leq$10 cm) were also pointed out [60,63]. It was reported that the gas holdup was not highly dependent on column diameter when the column diameter was larger than 10 cm, as long as mixing was well maintained. Daly et al. [64] found that the holdup is independent of the column height. Additionally, though not so significant, they obtained some differences in holdup with variation of the column diameter. It was observed that the holdup in small diameter column was slightly higher than that in larger diameter columns. The effect of column dimensions on gas holdup in foaming systems has not received significant attention in literature. Pino et al. [32] observed no appreciable differences in the gas holdup of foaming systems between columns of 10 and 29 cm in diameter, in the semibatch mode of operation. It was also reported that the effect of column height was insignificant for height to diameter ratios between 3 and 12. At high gas velocities when foaming occurred, both column height and diameter had no effect on gas holdup, whereas, for non-foaming systems and for column diameters up to 15 cm, gas holdup was found to decrease with increasing column diameter. According to the two-phase model developed by Krishna et al. [43,57,72] the effect of column diameter on gas holdup should be separately analyzed for small and large bubble gas holdups. It was found out that the small bubble gas holdup is independent of column diameter, while the large bubble gas holdup decreased with increasing column diameter. As a result the overall holdup is reported to decrease with increasing column diameter due to large bubble holdup. The dependence of large bubble holdup on column diameter was described by the following correlation proposed by Krishna et al. [43]:

$$\varepsilon_{b,lg} = \alpha_2 \frac{1}{D_T^N}(V_g - V_{df})^{0.58} \quad (3)$$

Here, $\varepsilon_{b,lg}$ is the holdup due to large bubbles which constitute the dilute-phase, α_2 and N fit parameters ($\alpha_2 = 0.268$ and $N = 0.18$ for gas–liquid systems and solid concentrations up to 16% by volume and $\alpha_2 = 0.3$ and $N = 0.18$ for higher solids concentrations), D_T the column diameter, V_g the superficial gas velocity entering the column and V_{df} is the superficial velocity of the dense-phase or the superficial velocity of large bubbles.

2.3.5. Gas sparger

Gas sparger type is an important parameter that can alter bubble characteristics which in turn affects gas holdup values and thus many other parameters characterizing bubble columns. The sparger used definitely determines the bubble sizes observed in the column. Small orifice diameter plates enable the formation of smaller sized bubbles. Some common gas sparger types that are used in literature studies are perforated plate, porous plate, membrane, ring type distributors and arm spargers. Bouaifi et al. [5] stated that, the smaller the bubbles, the greater the gas holdup values. Thus, they concluded that with small orifice gas distributors their gas holdup values were higher. In another study by Luo et al. [4], gas holdup was found to be strongly affected by the type of gas distributor. The effect was more pronounced especially for gas velocities below 6 cm/s. Schumpe and Grund [48] worked with perforated plate and ring type gas spargers. They concluded that with ring type distributor, the total holdup was smaller. They also added that the small bubble holdup showed a gradual increase with increasing superficial velocity with ring type sparger. Another conclusion about the type of spargers was that the contributions of both small and large bubbles to gas velocity were lower with ring sparger as compared to the perforated plate.

2.3.6. Solid concentration

The effect of solid concentration and particle size on gas holdup has been investigated by a number of researchers. Several researchers concluded that an increase in solids concentration generally reduced the gas holdup [32,43,60,66–69,74]. Sada et al. [69] also reported that for low solids loading (<5 vol.%), the behaviour of the slurry bubble column is close to that of a solid-free bubble column. Contrarily, Kara et al. [66] found a strong dependence of gas holdup on solids concentration at low solids concentrations. Kato et al. [74] reported that the effect of solid concentration on gas holdup becomes significant at high gas velocities (>10–20 cm/s).

Many studies have been conducted to investigate the effects of particle size on gas holdup as well [66,69,74]. The influence of particle size has been found to depend on a number of factors including flow regime, gas velocity, liquid properties and slurry concentration. It is generally reported that addition of solids to a two-phase system decreases the holdup [14,32,43,63,68]. For a fixed gas velocity and solid concentration, increasing the solid diameter also decreased the holdup and this effect of particle size was more pronounced for low concentration slurry systems [63]. Pino et al. [32] investigated foaming regime by using four different types of solid packings with various particle diameters. They observed that using coarser particles increased foaming and at high velocities, for all type of solid particles increasing the solid concentration reduced the gas holdup. In fact, the decrease of holdup in the presence of solid is attributed to decrease of small bubble holdup [43].

On the other hand, large bubble holdup is reported to be independent of solids concentration. Based on this, Krishna et al. [43] proposed a correlation for small bubble holdup showing its dependence on solids concentration:

$$\varepsilon_{df} = \varepsilon_{df,0}\left(1 - \frac{0.7}{\varepsilon_{df,0}}\phi_s\right) \quad (4)$$

Here, ε_{df} is the dense-phase gas holdup (small bubble holdup), $\varepsilon_{df,0}$ the gas holdup for only gas–liquid system, and ϕ_s is the solids volume fraction. The dense-phase gas holdup for the gas–liquid, $\varepsilon_{df,0}$, can be estimated using the correlation proposed by Reilley et al. [75] for the gas voidage at the regime transition point ε_{trans} as suggested by Krishna et al. [43,57]. Li and Prakash [14,68] reported a decrease in holdup with increasing solid concentration up to 25% by volume concentration. Afterwards, the gas holdup showed a slight increase. This unusual behaviour was attributed to the accumulation of fine bubbles at high slurry concentrations and decrease in the rise velocity of small bubbles.

There are very few studies in literature on the use of actual cells in slurry bubble columns as the solid phase, in contrast to many studies which report the decrease of gas holdup with solids concentration. In the study of Prakash et al. [3], holdup was observed to increase with solids concentration. During the operation of the column, it was observed that a foam layer was formed, at the top of the dispersion, due to the presence of surface active agents like alcohols, proteins, etc. in the solutions used. Increasing the yeast concentration just increased the surfactant concentration which in turn increased the foam bed and resulted in higher gas holdup values.

2.3.7. Summary of gas holdup studies

Summarizing the studies discussed so far about gas holdup it can be said that, the gas holdup increases with increasing gas velocity and operating pressure; whereas it decreases with increasing liquid viscosity and solid concentration. Adding a surface active reagent into the slurry increases the holdup. In bubble columns, the effect of column size on gas holdup is negligible when the column diameter is larger than 10–15 cm and the height is above 1–3 m, in other words with height to diameter ratios (aspect ratio) larger than 5. At low gas velocities, gas holdup depends on the number, pitch and diameter of the orifice holes. For orifice diameter larger than 1 mm, the effect of orifice diameter becomes insignificant.

2.4. Bubble characteristics

Bubble populations, their holdup contributions and rise velocities have significant impact on altering the hydrodynamics, as well as heat and mass transfer coefficients in a bubble column. For this reason it is important to obtain information on bubble properties of the slurry. Various studies proposed several methodologies to follow the estimation of bubble properties. In fact, all of these methods are based on two-bubble class model proposed by Krishna et al. [72]. Hence, bubble holdups and rise velocities are estimated for large and small bubble groups. Krishna and coworkers [57,72] proposed simplified equations that describe the bubble classes and behaviour in a bubble column operating in the churn-turbulent regime. Based on their correlation, given the regime transition properties between bubbly flow and churn-turbulent flow, namely the transition superficial velocity, $V_{g,trans}$ and transition (critical) holdup $\varepsilon_{g,trans}$, the small and large bubble velocities and holdup contributions can be estimated. Researches on bubble size distributions and factors affecting bubble sizes such as gas density, liquid viscosity, surface tension and operating conditions (pressure, temperature) are widely reported in literature [15]. Many literature correlations are proposed to predict the bubble holdups and their rise velocities and sizes of bubbles and most important ones are presented in Tables 5–7, respectively.

The dynamic gas disengagement (DGD) technique is a very widely adopted method to study bubble groups, bubble holdup structures and rise velocities. The principle involves tracing the drop in dispersion height after the gas flow has been shut off. The resulting disengagement profile can be used to separate the contributions of small and large bubbles to the total gas holdup [48]. The technique was first introduced by Stiram and Mann [76]. More specifically it requires an accurate measurement of the rate at which the level of gas–liquid dispersion drops after the gas flow to the bubble column is shut off [64]. The underlying idea in this technique is that different bubble classes in dispersion can be distinguished if there are significant differences between their rise velocities. Li and Prakash [14] reported that the rate at which the instantaneous gas holdup drops would depend on the fraction and rise velocities of different bubble classes. Thus, initially when the fast rising larger bubbles were escaping, a fast drop in gas holdup was observed. After the disengagement of large bubbles was completed, slower

Table 5
Correlations for small and large bubble holdups

Research group	Correlation	Reference
Krishna et al. [57,72]	Homogeneous regime: $\varepsilon_{g,hom} = \frac{V_g}{u_{b,sm}}$, heterogeneous regime $\varepsilon_{b,sm} = \varepsilon_{g,trans} = \frac{V_{g,trans}}{u_{b,sm}}$, $\varepsilon_{b,lg} = \frac{V_g - V_{g,trans}}{u_{b,lg}}$, $\varepsilon_{b,lg} = A(V_g - V_{g,trans})^n$	[57]
Ellenberger and Krishna [110]	$\varepsilon_{b,sm} = \varepsilon_{b,sm0}\left(1 - \frac{0.7}{\varepsilon_{b,sm0}}\phi_s\right)$; $\varepsilon_{b,lg} = \alpha_2 \frac{1}{D_T^N}(V_g - V_{g,trans})^{0.58}$, $V_{g,trans} = u_{b,sm}\varepsilon_{b,sm}$ with ϕ_s = slurry volume concentration, D_T = column diameter, $N = 0.18$, $\alpha_2 = 0.268$ for $\phi_s < 10\%$, $\alpha_2 = 0.3$ for $\phi_s > 10\%$	[43]

Table 6
Correlations for bubble rise velocity

Name	Correlation	Reference
Stoke's equation	$u_{b,small} = \frac{g\rho}{18\mu} d_b^2$ for $Re < 1$	[111]
Hadamard–Rybczynski equation	$u_b = \frac{g\rho}{18\mu} d_b^2$	[111]
Schügerl equation	$u_b = \left[\frac{\rho_l g}{K} \frac{2^{1+n}}{X_n} \left(\frac{4\pi}{3}\right)^{(2-n)3}\right]^{1/n} V_b^{(1+n)3n}$, X_n = (drag coefficient) $\left(\frac{\rho_l d_b^n u_b^{2-n}}{K}\right)$, $X = 24$ for Stoke's regime, $X = 16$ for Hadamard regime, $X = 48$ for Levich regime	[111]
Wilkinson equation	$\frac{u_{b,sm}\mu_l}{\sigma} = 2.25\left(\frac{\sigma^3\rho_l}{g\mu_l}\right)^{-0.273}\left(\frac{\rho_l}{\rho g}\right)^{0.03}$; $\frac{u_{b,lg}\mu_l}{\sigma} = \frac{u_{b,sm}\mu_l}{\sigma} + 2.4 \left(\frac{(V_g - V_{g,trans})\mu_l}{\sigma}\right)^{0.757}$, $\left(\frac{\sigma^3\rho_l}{g\mu_l^4}\right)^{-0.077}\left(\frac{\rho_l}{\rho g}\right)^{0.077}$, $\frac{V_{g,trans}}{u_{b,sm}} = 0.5\exp(-193\rho_g^{-0.61}\mu_l^{0.5}\sigma_l^{0.11})$	[57]
Equation proposed by Li and Prakash	$u_{b,sm} = u_{b,sm0}\left[1 + \frac{1.073}{u_{b,sm0}}\phi_s\right]$	[14]

moving small bubbles disengaged. However, the rate of drop in this period would slow down.

The average bubble size in a bubble column has been found to be affected by gas velocity, liquid properties, gas distribution, operating pressure and column diameter. The rise velocity of a single gas bubble depends on its size. Thus, the size and rise velocity of a bubble depend on each other and affected by the same parameters. In the following subsections, the results of various studies on bubble characteristics such as bubble size, rise velocity, bubble holdups are analyzed.

2.4.1. Superficial gas velocity

Due to the differences in the distributor design, column diameter and range of gas velocities studied, literature studies report different average bubble sizes and bubble rise velocities. The effect of gas flow rates on bubble size and bubble rise velocity was investigated by Akita and Yoshida [77] and a decrease in bubble size with increasing gas flow rate was reported. Contrarily, Fukuma et al. [78] and Saxena et al. [63] reported that the bubble sizes increased with increasing superficial gas velocity and at a certain gas velocity, maximum bubble size was attained. Similarly, Li and Prakash [14] reported that the bubble size increased with increasing superficial gas velocity. In the centre of the column larger bubbles were more dominant and smaller bubbles were collected in the near wall more densely. It was also reported that the contribution of small bubbles to overall holdup was more than the contribution of large bubbles. The rise velocity of small bubbles decreased with increasing superficial gas velocity, whereas the rise velocity of large bubbles increased with increasing superficial gas velocity [3]. Schumpe and Grund [48] also investigated the variation of the small and large bubble rise velocities with superficial gas velocity. They reported that the small bubble rise velocity decreased gradually as the superficial velocity was increased and the small bubble rise velocity attained an almost constant value afterwards. However, the large bubble rise velocity continuously increased with superficial gas velocity.

2.4.2. Liquid phase properties and operating conditions

The liquid properties also have a significant effect on bubble properties. The rise velocity of a single gas bubble depends on the size of the bubble. Thus, possible effects of liquid properties on bubble sizes would be also reflected in bubble rise velocities. The average bubble size was reported to decrease with decreasing surface tension of liquid [77] and increase with increasing liquid viscosity [68]. Luo et al. [4] investigated the effect of pressure on bubble dynamics and concluded that at elevated pressures bubble sizes were reduced. Enhanced pressures were also claimed to increase gas inertia and decrease the surface tension thus leading to reduced maximum stable bubble sizes. Schäfer et al. [15] carried out an experimental study based on bubble size distributions under industrial conditions. They investigated the effect of gas density, surface tension, liquid viscosity, sparger design and operating conditions on bubble sizes. The authors reported that as the liquid viscosity or surface tension decreased the stable bubble diameters also

Table 7
Correlations for the size of bubbles produced at an orifice

Researcher	Correlation	Reference
Miller [112]	$d_b = \left[\frac{6\sigma d_o}{g(\rho_l - \rho_g)}\right]^{1/3}$ for low gas flow rates	[111]
Moo-Young and Blanch [111]	$d_b = 0.19 d_o^{0.48} Re_o^{0.32}$, Re_o is the orifice Reynolds number and $Re_o = \frac{4Q\rho_g}{\pi d_o \mu_g}$	[111]
Leibson et al. [113]	$d_b = 0.18 d_o^{1/2} Re_o^{1/3}$ $Re < 2000$	[111]
Kumar and Kuloor [114]	$V_b = \left(\frac{4\pi}{3}\right)^{1/3}\left(\frac{15\mu_l Q}{2\rho_l g}\right)^{3/4}$	[111]
Bhavaraju et al. [115]	$\frac{d_b}{d_o} = 3.23\left(\frac{4\rho_l Q}{\pi\mu_l d_o}\right)^{-0.1}\left(\frac{Q^2}{d_o^5 g}\right)^{0.21}$	[111]

decreased. The influence of operating pressure and temperature were also discussed and it was observed that increasing temperatures or pressures resulted in reduced bubble sizes, which supported the findings of Luo et al. [4]. Veera et al. [11] carried out experiments with foaming liquids and reported that bubble sizes were reduced with increasing foaming agent concentrations.

2.4.3. Column dimensions

Although not commonly reported, the effect of column dimensions on bubble characteristics have been investigated by several researchers. Daly et al. [64] analyzed the sauter mean bubble diameters (mean surface to volume diameter) in two different bubble columns and reported that the column height was not effective. For gas velocities above 4 cm/s, the sauter mean bubble diameter was slightly higher in small diameter column. This was attributed to different flow regimes in the two columns at these velocities. The authors claimed that, at this superficial velocity the large diameter column operated in churn-turbulent regime where small bubbles were more dominant, because of the increased liquid circulation and turbulence in large diameter column. Under these conditions, the small diameter column operated in the slug flow regime where larger bubbles dominated. Li and Prakash [14] reported that the diameter of the column has an effect on the rise velocity of large bubbles only. They discovered that as the column diameter increased, the rise velocity of large bubbles also increased. Koide et al. [79] measured average bubble sizes in two columns with different diameters and a higher average bubble size was obtained in the larger diameter column.

2.4.4. Solid concentration

The presence of solids and solid concentration also has an impact on bubble properties. It was reported that the presence of solids led to larger bubble sizes [4,14,68]. This was attributed to an increase in the apparent slurry viscosity with increasing slurry concentration. The study by Krishna et al. [43] showed that the large bubble holdup was independent of solids concentration but the small bubble holdup was a decreasing function of solids concentration. Prakash et al. [3] utilized yeast cells in their column and reported that, as the yeast concentration increases, the rise velocity of large bubbles increases, whereas rise velocity of small bubbles decreases. This situation actually reflects the possible differences between actual cell particles and solid particles such as glass beads used in above-mentioned studies.

2.4.5. Summary of bubble characteristics studies

Summarizing so far, the published work discussed on bubble characteristics showed that the bubble sizes increase with increasing superficial gas velocity, solid concentration (up to a certain value), liquid viscosity and surface tension. On the other hand, the average bubble size was reported to decrease increasing foaming agent concentrations. Small bubble contribution to total holdup is essentially constant in churn-turbulent regime, being approximately equal to transition holdup. Large bubble holdup depends on the column diameter but not on solids concentration whereas for the small bubble holdup just the opposite is valid.

2.5. Mass transfer coefficient

The overall mass transfer rate per unit volume of the dispersion in a bubble column is governed by the liquid-side mass transfer coefficient, $k_l a$ assuming that the gas side resistance is negligible. In a bubble column reactor the variation in $k_l a$ is primarily due to variations in the interfacial area [59]. Assuming spherical bubbles, the specific gas–liquid interfacial area is related to the gas holdup, ε_g and the sauter mean bubble diameter, d_s by

$$a_s = \frac{6\varepsilon_g}{d_s} \tag{5}$$

Thus, a precise knowledge of the gas holdup and bubble size distribution is needed to determine the specific gas–liquid interfacial area [64]. In gas–liquid reactors, mass transfer from the gas to liquid phase is the most important goal of the process. The volumetric mass transfer coefficient is a key parameter in the characterization and design of both industrial stirred and non-stirred gas–liquid reactors. However, very few data are found dealing separately with mass transfer coefficient (k_l) and interfacial area in bubble columns or stirred reactors [5,80]. Most investigations performed are limited to the determination of the volumetric mass transfer coefficient, $k_l a$, which is the product of the liquid mass transfer coefficient 'k_l' and interfacial area 'a'. Unfortunately, this parameter is global and not sufficient to provide an understanding of the mass transfer mechanisms. The separation of the parameters 'k_l' and 'a' should be considered for better comprehension of the gas–liquid mass transfer mechanisms. It also allows us to identify which parameter (k_l or a) controls the mass transfer.

Since mass transfer is the key phenomenon in the chemical reactions taking place in the reactor, it is important to estimate the mass transfer coefficients for design and scale-up of these reactors. Literature studies are reviewed from the aspect of the effects of operational parameters on mass transfer characteristics and several important correlations to predict the mass transfer coefficient in bubble columns are presented in Table 8.

2.5.1. Superficial gas velocity

Krishna and Van Baten [30] developed a CFD model to describe mass transfer for air–water bubble column operating in both homogeneous and heterogeneous regime. The volumetric mass transfer, $k_l a$, increased with increasing gas velocity in the same trend as the gas holdup increased with superficial gas velocity. Verma and Rai [28] measured

Table 8
Mass transfer coefficient correlations for gas–liquid bubble columns

Research group	Correlation	Reference
Ozturk et al. [70]	$\frac{k_l a d_b^2}{D_{AB}} = 0.62\left(\frac{\mu_l}{\rho_l D_{AB}}\right)^{0.5}\left(\frac{g\rho_l d_b^2}{\sigma}\right)^{0.33}\left(\frac{g\rho_l^2 d_b^3}{\mu_l^2}\right)\left(\frac{V_g}{\sqrt{g d_b}}\right)^{0.68}\left(\frac{\rho_g}{\rho_l}\right)^{0.04}$, $Sh = 0.62 Sc^{0.5} Bo^{0.33} Fr^{0.68}\left(\frac{\rho_g}{\rho_l}\right)^{0.04}$	[70]
Akita and Yoshida [116]	$\frac{k_l a D_T^2}{D_{AB}} = 0.6\left(\frac{\upsilon_l}{D_{AB}}\right)^{0.5}\left(\frac{g D_T^2 \rho_l}{\sigma}\right)^{0.62}\left(\frac{g D_T^3}{\upsilon_l^2}\right)^{0.31}\varepsilon_g^{1.1}$	[6]
Shah et al. [2]	$k_l a = 0.467 V_g^{0.82}$	[6]
Kawase and Moo-Young [87]	$\frac{k_l a D_T^2}{D_{AB}} = 0.452\left(\frac{\upsilon_l}{D_{AB}}\right)^{1/2}\left(\frac{D_T V_g}{\upsilon}\right)^{3/4}\left(\frac{g D_T^2 \rho_l}{\sigma}\right)^{3/5}\left(\frac{V_g^2}{D_T g}\right)^{7/60}$	[6]
Hikita et al. [117]	$\frac{k_l a V_g}{g} = 14.9\left(\frac{V_g \mu_l}{\sigma}\right)^{1.76}\left(\frac{\mu_l^4 g}{\rho_l \sigma^3}\right)^{-0.248}\left(\frac{\mu_g}{\mu_l}\right)^{0.243}\left(\frac{\mu_l}{\rho_l D_{AB}}\right)^{-0.604}$	[27]
Kang et al. [118]	$k_l a = K \times 10^{-3.08}\left(\frac{D_T V_g \rho_g}{\mu_l}\right)^{0.254}$ where K is the correlation dimension	[27]
Schumpe and Grund [48]	$k_l a = K V_g^{0.82} \mu_{eff}^{-0.39}$, $K = 0.063$ (water/salt solution), $K = 0.042$ (water, 0.8 M Na_2SO_4)	[27]

the ionic mass transfer coefficient for electrolytic solutions in a bubble column using an electrochemical technique. A monotonic increase of the average mass transfer coefficient with gas velocity was observed. Letzel et al. [81] used the dynamic pressure-step method to measure $k_l a$ and found that the ratio of $k_l a$ to gas holdup was independent of superficial gas velocity for pressures up to 1 MPa. Behkish et al. [27] investigated the volumetric mass transfer coefficient and bubble size distribution for four different gas phases and in two different organic liquid mixtures and $k_l a$ values were also found to increase with gas velocity.

2.5.2. Liquid phase properties

Experiments performed with viscous media showed that the volumetric mass transfer coefficient, $k_l a$, decrease with increasing liquid viscosity [27,78]. It was pointed out that higher viscosity led to increase of the volume fraction of the large bubbles, leading to much lower gas–liquid interfacial areas. Ozturk et al. [70] investigated mass transfer coefficient in various organic liquids and observed that $k_l a$ values increased with increasing gas density. Interestingly, the authors reported that $k_l a$ values in mixed liquids were close to those in pure liquids of similar properties. Muller and Davidson [82] performed experiments with viscous media and pointed out the effect of surface active agents on the mass transfer. They reported that $k_l a$ values increase in the presence of surfactants. The authors attributed this increase to the creation of small bubbles and reduced bubble coalescence due to surfactants. Recently, Vandu and Krishna [31] reported experimental work on estimation of volumetric mass transfer coefficient in a bubble column. While most of the published work is restricted to low gas velocities, low slurry concentrations and small column diameters, the study of Vandu and Krishna [31] dealt with high slurry concentrations and high superficial gas velocities. They reported that $k_l a$ values closely followed the trend in gas holdup and that $k_l a/\varepsilon_g$ was found to depend on the liquid-phase Schmidt number.

2.5.3. Solid concentration

Mass transfer measurements were carried out in the transition and heterogeneous flow regimes. It was reported that $k_l a$ values decreased with increasing solid concentration [27,67]. At low solids concentrations $k_l a$ values increased with fine particles, whereas, the gas–liquid interfacial area decreased with increasing solid concentration [48,83]. Vandu and Krishna [31] observed that addition of solids and high solid concentrations caused reduced values of $k_l a/\varepsilon_g$ due to increased large bubble sizes.

2.5.4. Bubble properties

Fukuma et al. [78] suggested proportionality between the mass transfer coefficient values and volume–surface mean bubble diameter. Krishna and Van Baten [30] reported that in the heterogeneous regime the mass transfer was significantly enhanced by the continuous bubble break-up and coalescence tendencies. Behkish et al. [27] reported that at high solids concentrations, large bubbles were formed with bubble coalescence tendencies and they limited the mass transfer in the column. As a result the authors concluded that for industrial bubble columns, the presence of small bubbles should be preferred and the presence of large bubbles should be avoided for effective mass transfer rates.

2.5.5. Column dimensions, gas sparger and operating conditions

Vandu and Krishna [31] observed that $k_l a/\varepsilon_g$ showed a slight increase with column diameter. Krishna and Van Baten [30] carried out CFD simulations and showed that $k_l a$ decrease with column diameter. Verma and Rai [28] reported that the mass transfer coefficient was independent of initial bed height. Higher values were obtained with the spargers for which the gas holdup values were also higher, i.e. higher values of mass transfer coefficient were obtained with perforated plate distributor. Vafopulos et al. [84] investigated the mass transfer in an air–water bubble column at pressures from 0.1 to 1 MPa. They reported that pressure has no significant effect on gas holdup and volumetric liquid-

phase mass transfer coefficient. However, many studies report a significant effect of pressure on mass transfer rates. For instance, Wilkinson and Haringa [85] worked in the pressure range of 0.1–0.4 MPa and reported that both the interfacial area and volumetric mass transfer coefficient increase with pressure. Similarly, experiments in the pressure ranges 0.1–0.8 MPa showed that k_la values increased with increasing pressure [27,86]. This was attributed to the corresponding increase of the gas–liquid interfacial area. Still higher pressures (up to 5 MPa) were examined in the study of Maalej et al. [29] and it was reported that both interfacial area and the volumetric mass transfer coefficient (k_la) were affected by pressure, whereas the mass transfer coefficient (k_l) was independent of pressure. It was concluded that for a fixed gas mass flow rate, the interfacial area and the volumetric mass transfer coefficient decrease with increasing operating pressure. However, for a fixed pressure, they increase with increasing gas mass flow rates.

2.5.6. Summary of mass transfer studies

Summarizing the literature studies, it can be concluded that the volumetric mass transfer coefficient, k_la increases with gas velocity, gas density and pressure whereas decreases with increasing solid concentration and liquid viscosity. It is also concluded that the presence of surfactants increase k_la, due to small bubbles. Thus, presence of large bubbles should be avoided in industrial columns for effective mass transfer.

2.6. Heat transfer coefficient

Thermal control in bubble columns is of importance since in many chemical and biochemical processes, chemical reactions are usually accompanied by heat supply (endothermic) or removal (exothermic) operation. Therefore, turbulent heat transfer from the reactor wall and inserted coils to the liquid has been the topic of much research in the literature [87]. Bubble columns have been widely adopted in many industrial productions and operations due to high heat transfer rates [88]. The heat transfer rate in gas–liquid bubble columns is reported to be generally 100 times greater than in single phase flow [89]. Many hydrodynamic studies investigate the heat transfer between the heating objectives and the system flow to understand the effects of hydrodynamic structures on the heat transfer for improving the design and operation of bubble column reactors [24].

Literature studies reported on heat transfer measurements in two- and three-phase systems can be divided into: (1) estimation of bed-to-wall heat transfer coefficients, and (2) estimation of immersed object-to-bed heat transfer coefficients [89]. Bed-to-wall heat transfer was investigated in detail by Kato et al. [90]. The investigations of immersed object-to-bed heat transfer have been reported by a number of researchers [25,60,63,68].

Most of the previous studies on heat transfer in bubble columns concerned the steady-state time-averaged heat transfer of the object-to-bed and wall-to-bed [89,90]. However, measurements of instantaneous heat transfer coefficients provide more insight into bubble dynamics and mechanism of heat transfer. Chen et al. [26] reported that the use of average heat transfer coefficient causes the loss of information related to the effect of instantaneous bubble dynamics on heat transfer. Hence, the authors emphasized the importance of studying the instantaneous heat transfer in bubble columns under wide range of conditions for a comprehensive understanding of the heat transfer mechanism and reliable modeling to improve design and operation. Kumar et al. [91], Li and Prakash [13,23] and Cho et al. [25] are some of the recent studies based on local instantaneous heat transfer coefficient measurements.

Very few heat transfer data have been published on the biochemical studies with microbial media so far. Especially, studies with non-Newtonian fermentation media have not received considerable attention, despite its wide occurrence. Kawase and Moo-Young [87] developed a theoretical model, which accounts for both the Newtonian and non-Newtonian cases. Their model was based on turbulent heat transfer in bubble column reactors where the heat transfer enhancement due to shear-thinning of the media had been investigated.

Measurements of heat transfer coefficients in general require a heat source and measurements of surface and bed temperatures. To estimate the local instantaneous heat transfer coefficient h ($W/m^2\,^\circ C$) for a heated object-to-bed system for instance, the temperature difference between the probe surface and the bulk, ΔT (°C) and the corresponding heat transfer flux, Q (W/m^2) should be measured. The following relation can then be applied:

$$h = \frac{Q}{\Delta T} \tag{6}$$

Many literature correlations exist for estimation of heat transfer coefficient that can be applied to two-phase bubble columns and three-phase slurry bubble columns. Several of these correlations are presented in Table 9. The basic parameters affecting the heat transfer are mainly the superficial gas velocity, particle size and concentration, liquid viscosity, particle density, axial/radial location of the heat transfer probe and column dimensions.

2.6.1. Superficial gas velocity

The effect of gas velocity on heat transfer coefficients in two and three-phase systems have been widely investigated [3,60,63]. Generally, it was demonstrated that the introduction of gas into a liquid or liquid–solid bed enhances the turbulence in the medium and thus increases the heat transfer coefficients. Moreover, higher gas velocities just enhance the heat transfer more. Therefore, though the system properties, operating conditions and measurement techniques differ, many studies reported that the heat transfer coefficients increase with increasing superficial gas velocity

Table 9
Heat transfer correlations for bubble and slurry bubble columns

Research group	Correlation	Reference
Hikita et al. [117]	$St(Pr)^{2/3} = 0.411\left(\frac{V_g\mu_l}{\sigma}\right)^{-0.851}\left(\frac{\mu_l^4 g}{\rho_l\sigma_l^3}\right)^{0.308}$	[63]
Mersmann et al. [119]	$h = 0.12\left(\frac{g^2\rho_l}{\mu_l}\right)^{1/6}\left(\frac{\rho_l-\rho_g}{\rho_l}\right)^{1/3}(k_l\rho_l C_{pl})^{1/2}$ for $Ar\,Pr > 106$	[63]
Zehner [120]	$h = 0.18(1-\varepsilon_g)\left[\frac{k_l^2\rho_l^2 C_{pl}V_f^2}{d_b(\pi/6\varepsilon_g)^{1/3}\mu_l}\right]^{1/3}$, $V_f = \left[\frac{d_b(\pi/6\varepsilon_g)}{2.5}\left(\frac{\rho_l-\rho_g}{\rho_l}\right)gDV_g\right]^{1/3}$; $Nu = 350.8\,Re^{0.108}\left(\frac{d_p}{d_o}\right)^{0.05}$, for $1 < \frac{d_p}{d_o} < 5$	[63]
Saxena et al. [63]	$h = 0.12\left(\frac{g^2\rho_l}{\mu_l}\right)^{1/6}\left(\frac{\rho_l-\rho_g}{\rho_l}\right)^{1/3}(k_l\rho_l C_{pl})^{1/2}$	[63]
Kim et al. [92]	$h = 0.0722(k_l\rho_l C_{pl}\{[V_g(\varepsilon_g\rho_g + \varepsilon_l\rho_l + \varepsilon_s\rho_s)]g(\varepsilon_l\mu_l)^{-1}\}^{1/2})^{1/2}$	[63]
Deckwer [89]	$St = 0.1(Re\,Fr\,Pr^2)^{-0.25}$ where $St = \frac{h_w}{\rho_l C_p V_g}$, $Re = \frac{V_g d_p \rho_l}{\mu_l}$, $Fr = \frac{V_g^2}{gD_c}$, $Pr = \frac{C_p\mu_l}{k_l}$	[89]
Kast [121]	$St = 0.1(Re\,Fr\,Pr^2)^{-0.22}$	[89]
Kolbel and Langemann [122]	$St = 0.11(Re\,Fr\,Pr^{2.5})^{-0.22}$	[89]
Shaykhutdinov et al. [123]	$St = 0.11(Re\,Fr\,Pr^{2.5})^{-0.22}$	[89]
Steiff and Weinspach [124]	$St = 0.113(Re\,Fr\,Pr^2)^{-0.26}$	[89]
Suh and Deckwer [125]	$h = 0.1(k_l\rho_l C_{pl}\{[V_g(\varepsilon_s\rho_s + \varepsilon_l\rho_l + \varepsilon_g\rho_g)]g(\varepsilon_l\mu_b)^{-1}\}^{1/2})^{1/2}$ where $\mu_b = \mu_l\exp\left(\frac{2.5\upsilon_s}{1-0.609\upsilon_s}\right)$	[63]
Kawase and Moo-Young [87]	$St = 0.134(Re\,Fr\,Pr^{8/3})^{-0.25}$	[87]
Konsetov [126]	$St = 0.256(Re^{1/2}\,Fr^{1/3}\,Pr)^{-2/3}$	[87]

irrespective of the solid phase properties (diameter, shape, and concentration) or liquid phase properties (density, viscosity, etc.) [3,14,60,63,68]. Studies also showed that the rate of increase of heat transfer coefficients with gas velocity was more pronounced at low gas velocity, and more gradual at higher gas velocities.

2.6.2. Liquid phase properties

The effect of liquid phase properties on heat transfer, especially the impact of liquid viscosity has been reported in several studies. The heat transfer coefficient has been found to decrease with increasing liquid viscosity in three-phase fluidized systems [26,60,68,92] regardless of particle size. This was actually attributed to lower turbulence attained in the viscous media.

2.6.3. Solid size and concentration

The influence of particle size and concentration on heat transfer coefficient has been investigated by many researchers in both three-phase bubble columns and fluidized beds [14,60,63,68,93]. In three-phase fluidized beds, the heat transfer coefficient increased with particle size at low gas velocities (<5 cm/s). At higher gas velocities, it passed through a minimum value at a particle size of about 1.5 mm. In general, the effect of particle size on heat transfer coefficients was negligible at particle sizes larger than 3.0 mm, particularly at high gas velocities. Some studies reported that the heat transfer coefficients increased with increasing slurry concentrations [60,93]. The reason given for that was the alteration of thermo-physical properties of the slurry with the introduction of solids and also enhanced exchange rate of fluid elements on the heated surface of the probe due to motion of solid particles. Moreover, the alteration of the bubble properties with solid addition was also needed to be taken into account. Addition of solids and increasing the solids concentrations increase the bubble coalescence leading to the formation of larger size bubbles with higher rise velocities. As a matter of fact, addition of solids causes larger bubble sizes with induced velocities and thus higher heat transfer rates are likely to be obtained. On the other hand, Li and Prakash [68] reported an opposite trend with Deckwer et al. [60]. They reported that as solid concentration increased the heat transfer coefficient decreased. This was explained by the promotion of viscosity of the medium with increase of solid concentration which in turn resulted in the decrease of turbulence in the system.

2.6.4. Axial/radial location of the heat transfer probe

The position of the heat transfer probe in the column was also reported to alter the values of the heat transfer coefficient. Thus, several studies were performed by locating the heat transfer probe at various axial/radial locations in the column and determining the corresponding values of the heat transfer coefficients at those locations. In fact, the axial heat transfer measurement differences in the column stem from measurement distance to the gas distributor and radial differences from the bubble populations. Saxena et al. [63] compared the heat transfer coefficients at two different axial locations. The probes were at 2.9 and 0.52 m from the distributor. Their results indicated that the heat transfer coefficients at 2.9 m were systematically higher than at the 0.52 m. This was attributed to the influence of the distributor region. The height of 0.52 m from bottom was less than two times the column diameter (0.305 m) corresponding to the developing region for bubble growth and liquid phase flow pattern. The

influence of the distributor region is reported usually to extend up to three or four times the column diameter [94]. In the distributor region the bubble sizes are definitely smaller than the ones in the bulk region. This is due to the fact that the external pressure around the bubble decreases as the bubble rises up in the column. Thus, large bubbles would be more dominant away from the distributor. Since faster moving large bubbles would be more effective on heat transfer as compared to small bubbles, higher heat transfer coefficient values could be observed at the top sections of the column, i.e. away from the distributor as compared to the distributor region. Heat transfer measurements at different radial locations were carried out by Li and Prakash [68] and Prakash et al. [3]. It was reported that the column centre heat transfer coefficients were higher than the near wall heat transfer coefficients, due to the fact that large bubbles collect more dominantly at the centre. In addition to that, obviously there existed more turbulence in the centre as compared to near wall, due to possible wall effects.

2.6.5. Column dimensions and operating conditions

The effect of column diameter on heat transfer was investigated in detail by Saxena et al. [63]. The authors reported that heat transfer coefficients measured in a larger diameter slurry bubble column (30.5 cm) was greater than in a smaller diameter column (10.8 cm). They attributed this result to a higher mixing rate attained in the larger diameter column. Saxena et al. [63] also performed experiments to study the effect of bed temperature on heat transfer coefficient. It was reported that with increasing temperature the heat transfer coefficient also increased. This could be explained by the reduced liquid viscosity and enhanced turbulence maintained at higher temperatures. Chen et al. [26] investigated the effect of operating pressure on heat transfer characteristics. The authors observed that the heat transfer coefficients increased with increasing pressure.

2.6.6. Summary of heat transfer studies

Summarizing the studies discussed so far on heat transfer it can generally be concluded that the heat transfer coefficient increases with increasing temperature, superficial gas velocity, and particle size, but a decreasing function of liquid viscosity and particle density. Two opposing conclusions for the effect of solid concentration on heat transfer coefficient exist. Some studies [60,93] report that increased solid concentrations increases the heat transfer coefficient values, while some report the opposite [68]. The increase of the heat transfer coefficient with increasing solid concentration has been attributed to a corresponding increase of the slurry viscosity which results in greater bubble sizes and higher large bubble rise velocities and thus higher heat transfer rates. On the other hand, the contrary result obtained by Li and Prakash [68] was explained by the fact that turbulence is reduced by an increase in viscosity of the system. In fact the viscosity of the system by addition of inert bead-like solids would not change significantly especially at low concentrations however it can definitely be said that the presence of solids just promotes heat removal from the surface of the heated object and in a way that enhances the turbulence in the system. Axial profiles of heat transfer measurements indicate that the heat transfer coefficient in bulk region is higher than in the distributor region. The heat transfer coefficient in the centre of the column is greater than the near wall due to the fact that large bubbles collect at centre and they are more effective in enhancing heat transfer in the system.

Acknowledgement

This research was supported by the Boğaziçi University Research Fund through project B.A.P 04A501.

Appendix A

a_s	gas–liquid interfacial area
Ar	Archimeds number
Bo	Bond number
C_p	specific heat
C'_p	slurry specific heat
C_s	solid concentration
C_{s0}	solid concentration at column bottom
d	diameter
d_o	orifice diameter
d_b	bubble diameter
d_{bi}	size of bubble i
d_e	dimensionless bubble diameter
d_{max}	maximum bubble diameter
d_p	particle diameter
d_R	reactor diameter
d_S	sauter mean bubble diameter
D_c	column diameter
D_L	diffusion coefficient
D_T	tower diameter
F	flow number
Fr	Froude number
$\overline{Fr}$	Froude number for slurry phase
g	gravitational acceleration
Ga	Gallilei number
h	heat transfer coefficient
h_0	clear liquid height above transducer at time zero
h_I	clear liquid height above transducer in phase I
$h_{w\ max}$	maximum wall side heat transfer coefficient
H	distance
ΔH	height difference between the transmitters
k	thermal conductivity
k'	slurry thermal conductivity
k_l	liquid thermal conductivity
k_s	solid thermal conductivity
k_{sl}	slurry thermal conductivity

k_l	mass transfer coefficient
k_la	volumetric mass transfer coefficient
K	parameter in correlation
Mo	Morton number
n_i	number of bubbles of size d_{bi}
N	Krishna–Ellenberger fit parameter
Nu	Nusselt number
P	pressure
ΔP	pressure drop along bed
Pr	Prandtl number
$\overline{Pr}$	Prandtl number for slurry phase
P_v	energy dissipation rate
q	heat transfer rate
Q	heat flux
r	radial distance from column centre
R	radius of column
Re	Reynolds number ($V_g d_p \rho_l / \mu_l$)
Re_o	orifice Reynolds number
$\overline{Re}$	Reynolds number for slurry phase
Re_T	Reynolds number ($V_g D_c \rho_g / \mu_g$)
Sc	Schmidt number
Sh	Sherwood number
St	Stanton number
$\overline{St}$	Stanton number for slurry phase
T	temperature
ΔT	temperature difference
u_b	bubble rise velocity
$u_{b,lg}$	large bubble rise velocity
$u_{b,sm}$	small bubble rise velocity
$u_{b,sm0}$	small bubble rise velocity in gas–liquid system
u_G	mean superficial velocity
V_b	volume of bubble
V_{df}	dense-phase (small bubble) superficial gas velocity
V_g	superficial gas velocity
$V_{g,lg}$	large bubble superficial gas velocity
$V_{g,sm}$	small bubble superficial gas velocity
$V_{g,trans}$	transition superficial gas velocity
V_i	volume of bubble of size d_{bi}
V_l	superficial liquid velocity
V_t	total volume of the dispersion
V_∞	terminal rise velocity
Weber	Weber number

Greek letters

α	Krishna–Ellenberger fit parameter
ε_d	dilute-phase (large bubble) gas holdup
ε_{df}	dense-phase (small bubble) gas holdup
$\varepsilon_{df,0}$	dense-phase (small bubble) gas holdup for gas–liquid system
ε_g	gas holdup
ε_{gi}	gas holdup due to bubble i
$\varepsilon_g(t)$	instantaneous gas holdup
$\varepsilon_{g,hom}$	gas holdup in homogeneous regime
$\varepsilon_{g,heter}$	gas holdup in heterogeneous regime
$\varepsilon_{g,lg}$	large bubble gas holdup
$\varepsilon_{g,sm}$	small bubble gas holdup
$\varepsilon_{g,trans}$	transition gas holdup
ε_l	liquid holdup
ε_s	solid holdup
$\varepsilon_{s,0}$	small bubble holdup in gas–liquid system
μ	viscosity
μ_b	viscosity of slurry
μ_{eff}	effective viscosity of slurry
μ_g	viscosity of gas phase
μ_l	viscosity of liquid phase
μ_{sl}	viscosity of slurry phase
ρ	density
ρ_g	gas density
ρ_l	liquid density
ρ_s	solid density
ρ_{sl}	slurry density
σ	surface tension
σ_l	liquid-phase surface tension
υ	kinematic viscosity
υ_s	solid volume fraction
υ_{sl}	effective kinematic slurry viscosity
ϕ_l	volume fraction of liquid phase
ϕ_s	volume fraction of solid phase

Subscripts

av	average
b	bubble
B	dilute phase (large bubble holdup)
df	dense phase (small bubble holdup)
heter	heterogeneous regime
hom	homogeneous regime
lg	large bubble
sm	small bubble
trans	transition regime

References

[1] Degaleesan S, Dudukovic M, Pan Y. Experimental study of gas-induced liquid-flow structures in bubble columns. AIChE J 2001;47:1913–31.

[2] Shah YT, Godbole SP, Deckwer WD. Design parameters estimations for bubble column reactors. AIChE J 1982;28:353–79.

[3] Prakash A, Margaritis A, Li H. Hydrodynamics and local heat transfer measurements in a bubble column with suspension of yeast. Biochem Eng J 2001;9:155–63.

[4] Luo X, Lee DJ, Lau R, Yang G, Fan L. Maximum stable bubble size and gas holdup in high-pressure slurry bubble columns. AIChE J 1999;45:665–85.

[5] Bouaifi M, Hebrard G, Bastoul D, Roustan M. A comparative study of gas holdup, bubble size, interfacial area and mass transfer coefficients in stirred gas–liquid reactors and bubble columns. Chem Eng Process 2001;40:97–111.

[6] Shimizu K, Takada S, Minekawa K, Kawase Y. Phenomenological model for bubble column reactors: prediction of gas holdups and volumetric mass transfer coefficients. Chem Eng J 2000;78:21–8.

[7] Anabtawi MZA, Abu-Eishah SI, Hilal N, Nabhan NBW. Hydrodynamic studies in both bi-dimensional and three-dimensional bubble columns with a single sparger. Chem Eng Process 2002;1:1–6.

[8] Wang S, Arimatsu Y, Koumatsu K, Furumato K, Yoshimato M, Fukunaga K, et al. Gas holdup, liquid circulating velocity and mass

transfer properties in a mini-scale external loop airlift bubble column. Chem Eng Sci 2003;58:3353–60.
[9] Forret A, Schweitzer J-MM., Gauthier T, Krishna R, Scweich D. Influence of scale on the hydrodynamics of bubble column reactors: an experimental study in columns of 0.1, 0.4 and 1 m diameters. Chem Eng Sci 2003;58:719–24.
[10] Tang C, Heindel TJ. Time-dependent gas holdup variation in an air–water bubble column. Chem Eng Sci 2004;59:623–32.
[11] Veera UP, Kataria KL, Joshi JB. Effect of superficial gas velocity on gas hold-up profiles in foaming liquids in bubble column reactors. Chem Eng J 2004;99:53–8.
[12] Essadki H, Nikov I, Delmas H. Electrochemical probe for bubble size prediction in a bubble column. Exp Therm Fluid Sci 1997;14:243–50.
[13] Li H, Prakash A. Analysis of bubble dynamics and local hydrodynamics based on instantaneous heat transfer measurements in a slurry bubble column. Chem Eng Sci 1999;54:5265–71.
[14] Li H, Prakash A. Influence of slurry concentrations on bubble population and their rise velocities in three-phase slurry bubble column. Powder Technol 2000;113:158–67.
[15] Schäfer R, Marten C, Eigenberger G. Bubble size distributions in a bubble column reactor under industrial conditions. Exp Therm Fluid Sci 2002;26:595–604.
[16] Lapin A, Paaschen T, Junghans K, Lübbert A. Bubble column fluid dynamics, flow structures in slender columns with large-diameter ring-spargers. Chem Eng Sci 2002;57:1419–24.
[17] Ruzicka MC, Zahadnik J, Drahos J, Thomas NH. Homogeneous–heterogeneous regime transition in bubble columns. Chem Eng Sci 2001;56:4609–26.
[18] Buwa VV, Ranade VV. Dynamics of gas–liquid flow in a rectangular bubble column: experiments and single/multi-group CFD simulations. Chem Eng Sci 2002;57:4715–36.
[19] Michele V, Hempel DC. Liquid flow and gas holdup-measurement and CFD modeling for two-and-three-phase bubble columns. Chem Eng Sci 2002;57:1899–908.
[20] Dhotre MT, Ekambara K, Joshi JB. CFD simulation of sparger design and height to diameter ratio on gas hold-up profiles in bubble column reactors. Exp Therm Fluid Sci 2004;28:407–21.
[21] Thorat BN, Joshi JB. Regime transition in bubble columns: experimental and predictions. Exp Therm Fluid Sci 2004;28:423–30.
[22] Li H, Prakash A. Survey of heat transfer mechanisms in a slurry bubble column. Can J Chem Eng 2001;79:717–25.
[23] Li H, Prakash A. Analysis of flow patterns in bubble and slurry bubble columns based on local heat transfer measurements. Chem Eng J 2002;86:269–76.
[24] Lin TJ, Wang SP. Effects of macroscopic hydrodynamics on heat transfer in bubble columns. Chem Eng Sci 2001;56:1143–9.
[25] Cho YJ, Woo KJ, Kang Y, Kim SD. Dynamic characteristics of heat transfer coefficient in pressurized bubble columns with viscous medium. Chem Eng Process 2002;41:699–706.
[26] Chen W, Hasegawa T, Tsutsumi A, Otawara K, Shigaki Y. Generalized dynamic modeling of local heat transfer in bubble columns. Chem Eng J 2003;96:37–44.
[27] Behkish A, Men Z, Inga RJ, Morsi BI. Mass transfer characteristics in a large-scale slurry bubble column reactor with organic liquid mixtures. Chem Eng Sci 2002;57:3307–24.
[28] Verma AK, Rai S. Studies on surface to bulk ionic mass transfer in bubble column. Chem Eng J 2003;94:67–72.
[29] Maalej S, Benadda B, Otterbein M. Interfacial area and volumetric mass transfer coefficient in a bubble reactor at elevated pressures. Chem Eng Sci 2003;58:2365–76.
[30] Krishna R, Van Baten JM. Mass transfer in bubble columns. Catal Today 2003;79–80:67–75.
[31] Vandu CO, Krishna R. Volumetric mass transfer coefficients in slurry bubble columns operating in churn-turbulent flow regime. Chem Eng Process 2004;43:987–95.
[32] Pino LZ, Solari RB, Siuier S, Estevez LA, Yepez MM, Saez AE. Effect of operating conditions on gas holdup in slurry bubble columns with a foaming liquid. Chem Eng Commun 1992;117:367–82.
[33] Lefebvre S, Guy C. Characterization of bubble column hydrodynamics with local measurements. Chem Eng Sci 1999;54:4895–902.
[34] Arcuri EJ, Slaff G, Greasham R. Continuous production of thienamycin in immobilized cell systems. Biotechnol Bioeng 1986;28:842–9.
[35] Federici F, Petruccioli M, Miller MW. Enhancement and stabilization of the production of glucoamylase by immobilized cells of *Aureobasidium pullulans* in a fluidized bed reactor. Appl Microbiol Biotechnol 1990;33:407–9.
[36] Sun Y, Furusaki S. Effects of product inhibition on continuous acetic acid production by immobilized *Acetobacter aceti*: theoretical calculations. J Ferment Bioeng 1990;70(1):196–8.
[37] Rodrigues MTA, Vilaca PR, Garbuio A, Takagai M. Glucose uptake rate as a tool to estimate hybridoma growth in a packed bed bioreactor. Bioprocess Eng 1999;21:543–56.
[38] Bordonaro JL, Curtis WR. Inhibitory role of root hairs on transport within root culture bioreactors. Biotechnol Bioeng 2000;70:176–86.
[39] Son SH, Choi SM, Lee YH, Choi KB, Yun SR, Kim JK, et al. Large-scale growth and taxane production in cell cultures of *Taxus cuspidate* using a novel bioreactor. Plant Cell Rep 2000;19(6):628–33.
[40] Chang IS, Kim BH, Lovitt RW, Bang JS. Effect of partial pressure on cell-recycled continuous co fermentation by *Eubacterium limosium* kist612. Process Biochem 2001;37:411–21.
[41] Shiao TI, Ellis MH, Dolferus R, Dennis ES, Doran PM. Overexpression of alcohol dehydrogenase or pryruvate decarbosylase improves growth of hairy roots at reduced oxygen concentrations. Biotechnol Bioeng 2002;77:455–61.
[42] Ogbonna JC, Mashima H, Tanaka H. Scale up of fuel production from sugar beet juice using loofa sponge immobilized bioreactor. Bioresource Technol 2001;76:1–8.
[43] Krishna R, De Stewart JWA. Ellenberger J, Martina GB, Maretto C. Gas holdup in slurry bubble columns: effect of column diameter and slurry concentrations. AIChE J 1997;43:311–6.
[44] Deckwer WD, Schumpe A. Improved tools for bubble column reactor design and scale-up. Chem Eng Sci 1993;48:889–911.
[45] Hyndman CL, Larachi F, Guy C. Understanding gas-phase hydrodynamics in bubble columns: a convective model based on kinetic theory. Chem Eng Sci 1997;52:63–77.
[46] Hills JH. Radial non-uniformity of velocity and voidage in a bubble column. Ind Eng Chem Process Des Dev 1974;20:540–5.
[47] Fan LS. Gas–Liquid–Solid Fluidization Engineering. Boston: Butterworths; 1989.
[48] Schumpe A, Grund G. The gas disengagement technique for studying gas holdup structure in bubble columns. Can J Chem Eng 1986;64:891–6.
[49] Kawagoe K, Inoue T, Nakao K, Otake T. Flow-pattern and gas holdup conditions in gas-sparged contactors. Int J Chem Eng 1976;16:176–83.
[50] Matsuura A, Fan LS. Distribution of bubble properties in a gas–liquid–solid fluidized bed. AIChE J 1984;30:894–903.
[51] Wu Y, Ong BJ, Al-Dahhan MH. Predictions of gas hold-up profiles in bubble column reactors. Chem Eng Sci 2001;56:1207–10.
[52] Millies M, Mewes D. Interfacial area density in bubbly flow. Chem Eng Process 1999;38:307–19.
[53] Hibiki T, Ishii M. Two-group interfacial area transport equations at bubbly-to-slug flow transition. Nucl Eng Des 2000;202:39–76.
[54] Olmos E, Gentric C, Vial Ch. Wild G, Midoux N. Numerical simulation of multiphase flow in bubble column reactors. Influence of bubble coalescence and break-up. Chem Eng Sci 2001;56:6359–65.
[55] Hills JH. The operation of a bubble column at high throughputs and gas holdup measurement. Chem Eng J 1976;12:89–99.

[56] Miller DN. Gas holdup and pressure drop in bubble column reactors. Ind Eng Chem Process Des Dev 1980;19:371–7.
[57] Krishna R, De Stewart JWA, Hennephof DD, Ellenberger J, Hoefsloot HCJ. Influence of increased gas density on hydrodynamics of bubble column reactors. AIChE J 1994;40:112–9.
[58] Bukur DB, Daly JG. Gas holdup in bubble columns for Fischer–Tropsch synthesis. Chem Eng Sci 1987;42:2967–9.
[59] Fan LS, Matsuura A, Chern SS. Hydrodynamic characteristics of a gas–liquid–solid fluidized bed containing a binary mixture of particles. AIChE J 1985;31:1801–10.
[60] Deckwer WD, Louisi Y, Zaidi A, Ralek M. Hydrodynamic properties of the Fisher–Tropsch slurry process. Ind Eng Chem Process Des Dev 1980;19:699–708.
[61] Hikita H, Asal S, Tanigawa K, Segawa K, Kitao M. Gas holdup in bubble column. Chem Eng J 1980;20:59–67.
[62] Reilley IG, Scott DS, De Bruijin T, Jain A, Piskorz J. A correlation for gas holdup in turbulent coalescing bubble columns. Can J Chem Eng 1986;64:705–17.
[63] Saxena SC, Rao NS, Saxena AC. Heat-transfer and gas-holdup studies in a bubble column: air–water–glass bead system. Chem Eng Commun 1990;96:31–55.
[64] Daly JG, Patel JG, Bukur DB. Measurement of gas holdups and sauter mean bubble diameters in bubble column reactors by dynamic gas disengagement method. Chem Eng Sci 1992;47:3647–54.
[65] Lockett MJ, Kirkpatrick RD. Ideal bubbly flow and actual flow in bubble columns. Trans Inst Chem Eng 1975;53:267–73.
[66] Kara S, Kelkar BG, Shah YT, Carr NL. Hydrodynamics and axial mixing in a three-phase bubble column. Ind Eng Chem Process Des Dev 1982;21:584–94.
[67] Koide K, Takazawa A, Komura M, Matsunga H. Gas holdup and volumetric liquid phase mass transfer coefficient in solid-suspended bubble column. J Chem Eng Jpn 1984;17:459–66.
[68] Li H, Prakash A. Heat transfer and hydrodynamics in a three-phase slurry bubble column. Ind Eng Chem Res 1997;36:4688–94.
[69] Sada E, Katoh S, Yoshil H. Performance of the gas–liquid bubble column in molten salt systems. Ind Eng Chem Process Des Dev 1984;23:151–4.
[70] Ozturk SS, Schumpe A, Deckwer WD. Organic liquids in a bubble column: holdups and mass transfer coefficients. AIChE J 1987;33:1473–80.
[71] Wilkinson PM, Spek AP, Van Dierendonck LL. Design parameters estimation for scale-up of high-pressure bubble columns. AIChE J 1992;38:544–54.
[72] Krishna R, Wilkinson PM, Van Dierendonck LL. A model for gas holdup in bubble columns incorporating the influence of gas density on flow regime transitions. Chem Eng Sci 1991;46:2491–6.
[73] Lin TJ, Tsuchiya K, Fan LS. Bubble flow characteristics in bubble columns at elevated pressure and temperature. AIChE J 1998;44:545–50.
[74] Kato Y, Nishiwaki A, Kago T, Fukuda T, Tanaka S. Gas holdup and overall volumetric absorption coefficient in bubble columns with suspended solid particles. Trans Inst Chem Eng 1973;13:562–7.
[75] Reilley IG, Scott DS, De Brujin TJW. MacIntyre D. The role of gas phase momentum in determining gas holdup and hydrodynamic flow regimes in bubble column operations. Can J Chem Eng 1994; 72:3.
[76] Stiram K, Mann R. Dynamic gas disengagement: a new technique for assessing the behavior of bubble columns. Chem Eng Sci 1977;32:571–80.
[77] Akita K, Yoshida F. Bubble size, interfacial area and liquid-phase mass transfer coefficient in bubble columns. Ind Eng Chem Process Des Dev 1974;12:76–80.
[78] Fukuma M, Muroyama K, Morooka S. Properties of bubble swarm in a slurry bubble column. J Chem Eng Jpn 1987;20:28–33.
[79] Koide K, Morooka S, Ueyama K, Matsuura A. Behavior of bubbles in large scale bubble column. J Chem Eng Jpn 1979;12:98–104.
[80] Kawase Y. The energy dissipation rate concept for turbulent heat and mass transfer in drag-reducing fluids. Int Commun Heat Mass Trans 1990;17(2):155–66.
[81] Letzel H, Shouten MJC. Krishna R, Van Den bleek CM. Gas holdup and mass transfer in bubble column reactors operated at elevated pressure. Chem Eng Sci 1999;54:2237–46.
[82] Muller FL, Davidson F. On the effects of surfactants on mass transfer to viscous liquids in bubble columns. Chem Eng Res Des 1995;73:291.
[83] Quicker G, Schumpe A, Deckwer WD. Gas–liquid interfacial areas in a bubble column with suspended solids. Chem Eng Sci 1984;39: 179.
[84] Vafopulos I, Sztatescny K, Moser F. Der einfluβ des partial-und gesamtdruckes auf den stoffaustausch. Chem Eng Technol 1975;47:681–786.
[85] Wilkinson P, Haringa H. Mass transfer and bubble size in a bubble column under pressure. Chem Eng Sci 1994;49(9):1417–27.
[86] Dewes I, Kuksal A, Schumpe A. Gas density effect on mass transfer in three-phase sparged reactors. Chem Eng Res Des 1995;73: 697.
[87] Kawase Y, Moo-Young M. Heat transfer in bubble column reactors with Newtonian and non-Newtonian fluids. Chem Eng Res Des 1987;65:121–6.
[88] Deckwer WD. Bubble Column Reactors. New York: Wiley; 1992.
[89] Deckwer WD. On the mechanism of heat transfer in bubble column reactors. Chem Eng Sci 1980;35:1341–6.
[90] Kato Y, Uchida K, Kago T, Morooka S. Liquid holdup and heat transfer coefficient between bed and wall in liquid–solid and gas–liquid–solid fluidized beds. Powder Technol 1981;28:173–9.
[91] Kumar S, Kusakabe K, Raghuathan K, Fan LS. Mechanism of heat transfer in bubbly liquid and liquid–solid systems: single bubble injection. AIChE J 1992;38:733–41.
[92] Kim SD, Kang Y, Kwon HK. Heat transfer characteristics in two- and three-phase slurry fluidized-beds. AIChE J 1986;32:1397–400.
[93] Kolbel H, Borchers E, Martins J. Warmeubergang in blasensaulen. III. Messungen an gasdurchstromten suspensionen. Chem Eng Tech 1960;32:84–8.
[94] Yamashita F. Effect of liquid depth, column inclination and baffle plates on gas holdup in bubble columns. J Chem Eng Jpn 1985;18:349–63.
[95] Joshi JB, Deshpande NS, Dinkar M, Phanikumar DV., editors. Hydrodynamic stability of multiphase reactors. Adv Chem Eng 2001;26:3–127.
[96] Bach HF, Pilhofer T. Variation of gas hold-up in bubble columns with physical properties of liquids and operating parameters of columns. Ger Chem Eng 1978;5:270–5.
[97] Oels U, Lucke J, Buchholz R, Schugerl K. Influence of gas distributor type and composition of liquid on the behavior of a bubble column bioreactor. Ger Chem Eng 1978;1:115–29.
[98] Yamashita F, Inoue H. Gas holdup in bubble columns. J Chem Eng Jpn 1975;8:444–9.
[99] Joshi JB, Sharma MM. A Circulation cell model for bubble columns. Trans Inst Chem Eng 1979;57:244–51.
[100] Kumar A, Dageleesan TE, Ladda GS. Bubble swarm characteristics in bubble columns. Can J Chem Eng 1976;54:503–8.
[101] Grover GS, Rode CV, Chaudrai RV. Effect of temperature on flow regimes and gas holdup in a bubble column. Can J Chem Eng 1986;64:501–4.
[102] Zou R, Jiang X, Li B, Zu Y, Zhang L. Studies on gas holdup in a bubble column operated at elevated temperatures. Ind Eng Chem Res 1988;27:1910–6.
[103] Hughmark GA. Holdup and mass transfer in bubble columns. Ind Eng Chem Process Des Dev 1967;6:218–20.
[104] Kawase Y, Umeno S, Kumagai T. The prediction of gas hold-up in bubble column reactors: Newtonian and non-Newtonian fluids. Chem Eng J 1992;50(1):1–7.

[105] Hikita H, Kikukawa H. Liquid phase mixing in bubble columns. Effect of liquid properties. Chem Eng J 1974;8:191.
[106] Godbole SP, Honath MF, Shah YT. Holdup structure in highly viscous Newtonian and non-Newtonian liquids in bubble columns. Chem Eng Commun 1982;16:119–34.
[107] Schumpe A, Deckwer WD. Viscous media in tower bioreactors: Hydrodynamic characteristics and mass transfer properties. Bioprocess Eng 1987;2:79–94.
[108] Smith DN, Fuchs W, Lynn RJ, Smith DH, Hess M. Bubble behavior in a slurry bubble column reactor model, chemical and catalytic reactor modeling. ACS Symp Ser 1984;237:125.
[109] Roy NK, Guha DK, Rao MN. Fractional gas holdup in two-phase and three-phase batch-fluidized bubble-bed and foam-systems. Indian Chem Eng 1963;27–31.
[110] Ellenberger J, Krishna R. A unified approach to the scale-up of gas–solid fluidized bed and gas–liquid bubble column reactors. Chem Eng Sci 1994;49:5391.
[111] Moo-Young M, Blanch HW. Design of biochemical reactors. Adv Biochem Eng 1981;19:1–69.
[112] Miller DN. Scale-up of agitated vessels gas–liquid mass transfer. AIChE J 1974;20:445–53.
[113] Leibson I, Halcomb EG, Cacosco AG, Jamic JJ. Rate of flow and mechanics of bubble formation from single submerged orifices. AIChE J 1956;2(3):296–306.
[114] Kumar R, Kuloor NR. The formation of bubbles and drops. Adv Chem Eng 1970;8:256–368.
[115] Bahavaraju SM, Mashelkar RA, Blanch HW. Bubble motion and mass transfer in non-Newtonian fluids. AIChE J 1978;24:1063–76.
[116] Akita K, Yoshida F. Gas hold-up and volumetric mass transfer coefficients in bubble columns. Ind Eng Chem Process Des Dev 1973;12:76–80.
[117] Hikita H, Asal S, Kikukawa H, Zalke T, Ohue M. Heat transfer coefficient in bubble column. Ind Eng Chem Process Des Dev 1981;20:540–5.
[118] Kang Y, Cho YJ, Woo KJ, Kim SD. Diagnosis of bubble distribution and mass transfer in pressurized bubble columns with viscous liquid medium. Chem Eng Sci 1999;54:4887.
[119] Mersmann A, North H, Wunder R. Maximum heat transfer in equipment with dispersed two-phase systems. Int J Chem Eng 1982;22:16–29.
[120] Zehner P. Momentum, mass and heat transfer in bubble columns. Trans Inst Chem Eng 1986;26:29–35.
[121] Kast W. Analyse des warmeubergangs in blasensaulen. Int J Heat Mass Trans 1962;5:329–36.
[122] Kolbel H, Langemann H. Warmeubergang in Blasensaulen. Erdol-Zeirschr 1964;80(10):405–15.
[123] Shaykhutdinov AG, Bakirov NU, Usmanov AG. Determination and mathematical correlation of heat transfer coefficient under conditions of bubble flow, cellular and turbulent foam. Int Chem Eng J 1975;11:641–5.
[124] Steiff A, Wienspach PM. Heat transfer in stirred and non-stirred gas–liquid reactors. Ger Chem Eng 1978;1:150–61.
[125] Suh IS, Deckwer WD. Unified correlation of heat transfer coefficients in three-phase fluidized beds. Chem Eng Sci 1989;44:1455–8.
[126] Konsetov VV. Heat transfer during bubbling of gas through liquid. Int J Heat Mass Trans 1966;9:1103–8.